NEAR EAST UNIVERSITY

Faculty of Engineering

Department of Electrical and Electronic Engineering

COMMUNICATION CHANNELS

Graduation Project
EE- 400

Student: Atiq-ur-Rehman Khan (960911)

Supervisor: Prof.Dr.Fakhreddin Mamedov

NICOSIA - 2002

ACKNOWLEDGMENT

First of all I like to thanks God for the courage, He gave me for the completion of my project and engineering.

Secondly I wish to thanks my parents who supported and inculcated me the sprit to learn more and more and who still being generous for me as they are ever.

I would like to thanks my honorable supervisor Prof. Dr. Fakhreddin Mamedov also who was very generous with his help, valuable advices to accomplish this project and who will be always my respectful teacher.

All my thanks goes to N.E.U educational staff especially to there electrical and electronic engineering teaching staff for their generosity and special concern of me and all E.E students,

Final acknowledge goes to my class mates and friends Shafiq, Shakeel, Azeem, khurram, Dawood, Ayoub, Raja saqib and Jehanzeb who provided me with their valuable suggestions throughout the completion of my project.

ABSTRACT

A communication channel is central to the operation of a communication system. Its properties determine goes the information carrying capacity of the system and the quality of service offered by the system. We may classify communication channel in different ways:

. A channel may be linear or nonlinear; a telephone channel is linear, wheras a satellite channel usually (but not always) nonlinear.

. A channel may be time invariant or time varying; an optical fiber is time invarent, whereas a mobile radio channel is time varying.

. A channel may be bandwidth limited or power limited (i.e., limited in the available transmitted power); a telephone channel is bandwidth limited, whereas an optical fiber link and a satellite channel are both power limited.

The main objective this project is analysis and systematically information achieve of communication channels those bridge transmissions and receivers of communication system.

INTRODUCTION

In this project communication channels analysis can be classify into four channels, Telephone and Mobile Radio channels, Fiber Optic channel and Satellite channel. These four different channels for special attention because of their important roles in today's telecommunications environment, which can only grow with time.

The project consists of four chapters.

Chapter 1 gives a short introduction to communication channels analysis by considering the historical development, the general mathematical methods, Transmission Impairments, Channel Capacity.

Chapter 2 gives a short introduction to telephone and mobile radio channels. In telephone channel, gives basic ideas of works, connection to the central office, process a call the switch performs three main functions are explained. Digital switches, administration module are discussed, switch module, remote switch module. Finally, in mobile radio channel, building penetration losses, propagation inside buildings, radio propagation in tunnels are discussed in detail.

Chapter 3 short introduction to fiber optic channel, basic idea of optic fiber, attenuation and dispersion in fibers. Dispersion and pulse shaping in fibers undergoing diffusion, pulse stretching in multimode fibers are explained. Communication link models for the fiber channel are described.

Chapter 4 a short introduction to satellite channel, electromagnetic field propagation, the basic types and parameters of antennas are explained in detail. Finally, cover the important satellite links, satellite uplink, satellite downlink, repeater link, satellite crosslink, deep-space link are discussed in detail.

TABLE OF COTTENTS

1. INTRODUCTION TO COMMUNICATION CHANNELS

1.1 Introduction

The communication channel is the physical medium that connects the transmitter to the receiver. The physical channel may be a pair of wires that carry the electrical signals, or an optical fiber that carries the information on a modulated light beam or free space at which the information - bearing signal is electromagnetic waves.

Telephone and mobile radio channels, fiber optic channel, and satellite channel. These four different channels for special attention because of their important roles in today's telecommunications environment, which can only grow with time.

The first telegraph lines linked Washington with Baltimore and became operational in May 1844. An important milestone in telegraphy was the installation of the first transatlantic cable in1858 that linked the United States and Europe. It was not until 1953, when the first transatlantic cable was laid, and telephone service became available between the United States and Europe in 1895 Marconi and Popov demonstrated the transmission of radio signals at a distance of 2 kilometers. Currently, most of the wire line communication systems are being replaced by fiber optic cables which provide extremely high bandwidth and make possible transmission of a wide variety of information sources, including voice, data, and video.

The first communication from an artificial satellite took place in October 1957, when a Soviet satellite "Sputnik" transmitted elementary information, for 21 days. The first satellite used for voice communication was "Score", launched in December 8, 2001and used to broadcast President Eisenhower Christmas message. A satellite named Telstar was launched in 1962 and used to relay TV signals between Europe and the United States.

1.2 Mathematical Models for Communication Channels

In the design of communication systems we find it convenient to construct mathematical r that reflect the most important characteristics of the transmission medium. Below, we pro brief description of the channel models that are frequently used to characterize many of the pt channels that we encounter in practice.

1.2.1 The additive noise channel.

The simplest mathematical model for a communication channel is the additive noise channel, illustrated in Figure 1.1.

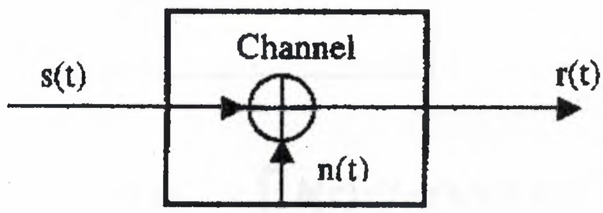

Figure 1.1 The additive noise channel

In this model, the transmitted signal s *(t)* is corrupted by an additive random noise pi *n (t)*. Physically, the additive noise process may arise from electronic components and amplify the receiver of the communication system, or from interference encountered in transmission the case of radio signal transmission.

If the noise is introduced primarily by electronic components and amplifiers at the race it may be characterized as thermal noise. This type of noise is characterized statistically *Gaussian noise process*. Hence, the resulting mathematical model for the channel is usually called the *additive Gaussian noise channel*. In this case the received signal is

$$r(t) = \alpha s(t) + n(t) \qquad (1.1)$$

Where a represent attenuation factor.

1.1.2 The linear filter channel

In some physical channels such as wire line tale: channels, filters are used to ensure that the transmitted signals do not exceed specified bandwidth limitations and thus do not interfere with one another. Such channel (Figure 1.2) output can be characterized as

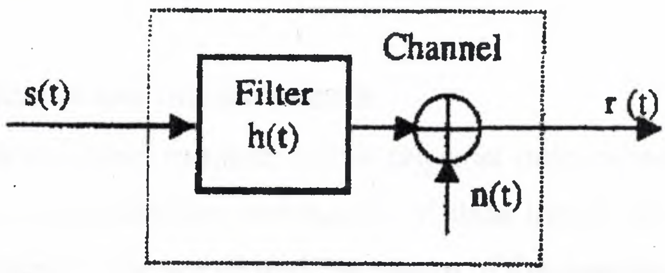

$$r(t) = s(t) * h(t) + n(t) = \int_{-\infty}^{\infty} h(\tau)s(t-\tau)d\tau + n(t) \quad (1.2)$$

Figure 1.2 The linear filter channel

Where h (t) is the impulse response of the linear filter and symbol * denotes convolution.

1.1.3 The linear time - variant filter channel

Physical channels such as underwater acoustic channels and ionosphere Radio channels, which result in time-variant multipart propagation of the transmitted signal, may be characterized mathematically as time-variant linear filters. Such system is characterized by a time-variant channel with impulse response h (τ ; t) filters (Figure 1.3). For an Input signal s (t), the channel output is

$$r(t) = s(t) * h(\tau; t) + n(t) \quad (1.3)$$

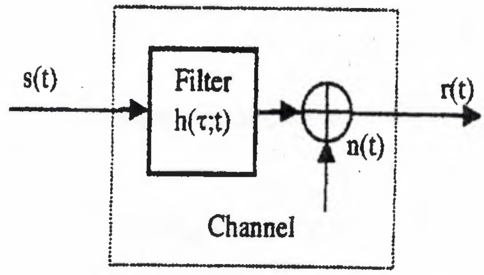

Figure 1.3 A linear time – variant filter channel

The three mathematical models described above adequately characterize a majority of physical channels encountered in practice.

1.3 Transmission Impairments

The transmission medium is the physical path between transmitter and receiver. The characteristics and quality of data transmission are determined both by the nature of the signal and the nature of the medium.

With any communication system, it must be recognized that the signal that is received will differ from the signal that is transmitted due to various transmission impairments. For analog signals, these impairments introduce various random modifications that degrade the signal quality. For digital signals, bit errors are introduced: a binary 1 is transformed into a binary 0 and vice versa.

The most significant impairments are: Attenuation, Delay distortion and Noise. The various impairment effects that can degrade a signal during transmission are shown in Figure 1.4.

1.3.1 Attenuation

As a signal propagate along a transmission medium its amplitude decreases. This is known as signal attenuation. To compensate the attenuation, amplifiers are inserted at intervals along the cable to restore the received signal to its original level. Signal attenuation increases as a function of frequency. To overcome this problem, the amplifiers are designed to amplify different frequency by varying gains of amplifications. These devices are known as equalizer. For guided media (Twisted wires. Coaxial cables and Fire optic cables) attenuation, is generally logarithmic and it is typically expressed as a constant number of decibels per unit distance

N, dB = 10log p2/p1, whereN – number of decibels (1.4)

P_1, P_2 - input and output powers, taking into account that power is proportional to the square of voltage:

$$P_1 = U^2{}_1/R \quad ; \quad P_2 = U^2{}_2/R \qquad (1.5)$$

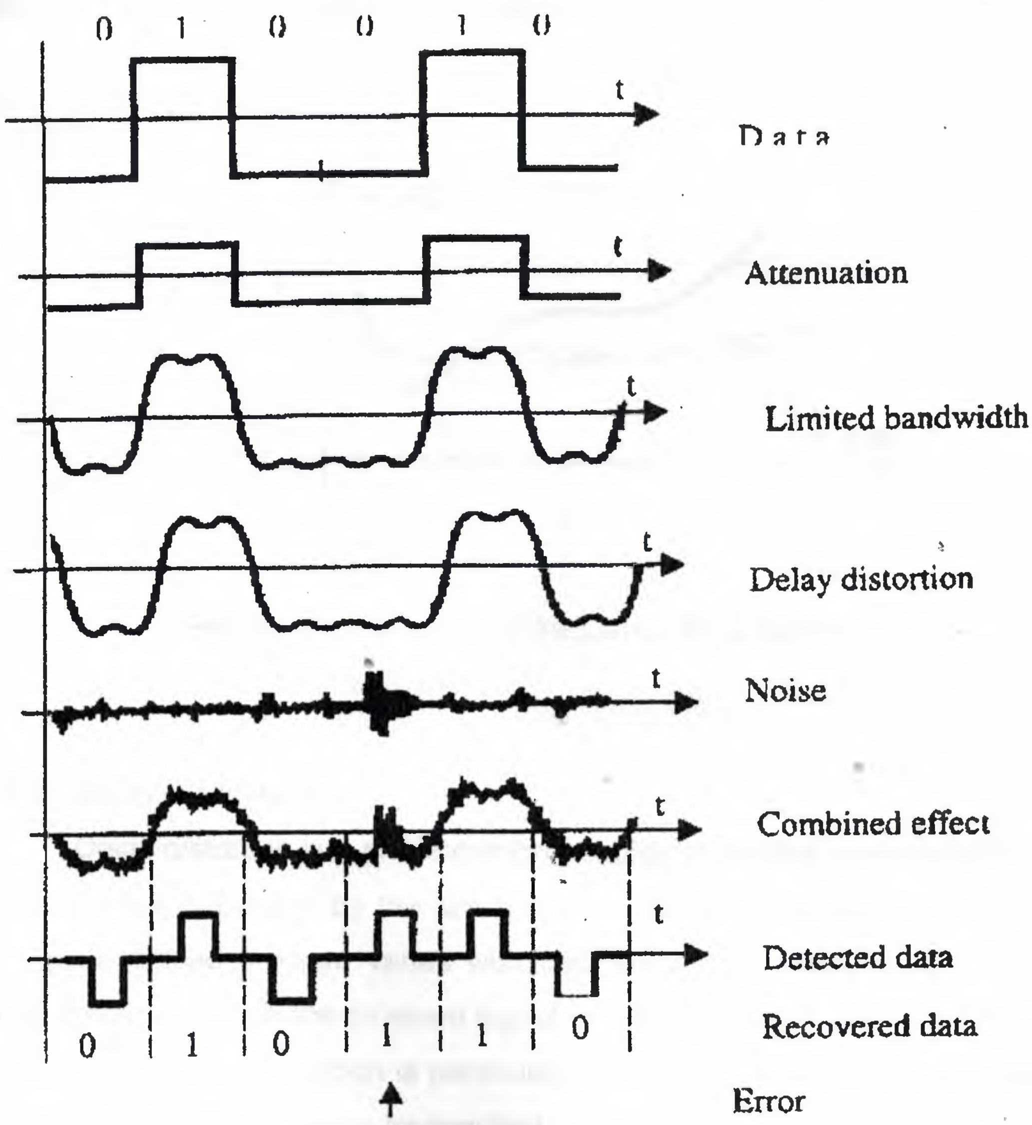

Figure 1.4 Degrade a signal during transmission

$$N, dB = 20\log U_2 / U1 \quad (1.6)$$

For unguided media attenuation is a more complex function of distance and the make-up of the atmosphere. An example is shown in Figure.1.4, which shows attenuation as a function of frequency for a typical wire line. In Figure, 1.4, attenuation is measured relative to the attenuation at 1000 Hz. Positive values on the y-axis represent attenuation greater than that at 1000 Hz. For another frequency f, the relative attenuation in decibels is $N_f = 10 \log_{10} P_f / P_{1000}$. The solid line in Figure.1.4 shows attenuation without equalization. The dashed line shows the effects of equalization.

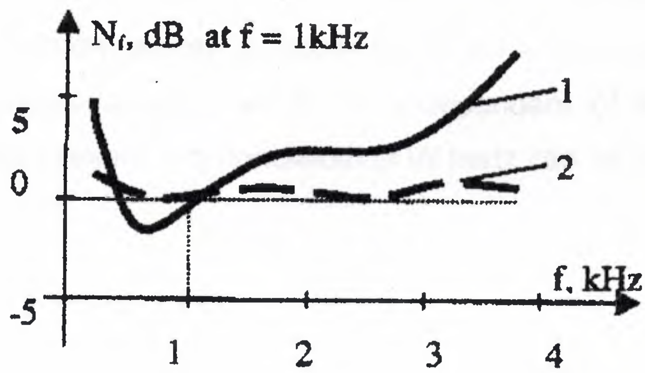

Figure 1.4 A function of frequency for a typical wire line

1.3.2 Delay Distortion

Delay distortion is a phenomenon peculiar to guided transmission media. The distortion is caused by the fact that the velocity of propagation of a signal through a guided medium varies with frequency. This effect is referred to as delay distortion, since the received signal is distorted due to variable delay in its components. Delay distortion is particularly critical for digital data. Consider that a sequence of bits is being transmitted, using either analog or digital signals. Because of delay distortion, some of the signal components of one bit position will spill over into other bit positions, causing inter symbol interference, which is a major limitation to maximum bit rate over a transmission control. Equalizing techniques can also be used for delay distortion.

1.3.3 Noise

For any data transmission, the received signal will consist of the transmitted signal, modified by the various distortions imposed by the transmission system, plus additional unwanted signals that are inserted somewhere between transmission and reception. These undesired signals are referred to *Noise* and can be divided into four categories: Thermal noise, Intel-modulation noise. Crosstalk and Impulse noise.

The Thermal noise is due to thermal agitation of electrons in a conductor. It is present in all electronic devices and transmission media and is a function of temperature. Thermal noise is uniformly distributed across the frequency spectrum and hence is often referred to as *white noise.* Thermal noise cannot be eliminated and therefore places an upper bound on communications system performance. This noise is assumed to be independent of frequency. The thermal noise in watts present in a bandwidth of W hertz can be expressed as

$$N = kTW \tag{1.7}$$

Or, in decibel – watts:

$$N = 10 \log k + 10 \log T + 10 \log W$$

$$N = -228.6\ (dbW) + 10 \log T + 10 \log W$$

Where No – noise power density, watts /hertz;

K – Boltzmann's constant $k = 1.3803 \times 10^{-23}$ j /° K; T – temperature, degrees Kelvin

When signals at different frequencies share the same transmission medium, the result may be *intermediation noise.* The effect of intermediation noise is to produce signals at a frequency, which is the sum or difference of the two original frequencies or multiples of those frequencies. For example, the mixing of signals at frequencies f_1 and f_2 might produce energy at the frequency $f_1 + f_2$.This derived signal could interfere with an intended signal at the frequency $f_1 + f_2$.

Intermodulation noise is produced when there is some nonlinearity in the transmitter, receiver, or interviewing transmission system.

Crosstalk has been experienced by anyone who, while using the telephone, he/she is able to hear another conversation: it is an unwanted coupling between signal paths. It can occur by electrical coupling between nearby twisted pair or rarely coaxial cable lines carrying multiple signals. Among several types of crosstalk the most limiting impairment for data communication systems is near end crosstalk (self-crosstalk or echo), since it is caused by the strong signal output by the transmitter output being coupled with much weaker signal at the input of the local receiver circuit. Adaptive noise canceller is used to overcome this type of impairment.

An *Impulse noise,* has short duration and of relatively high amplitude. It is generated from a variety of causes, including external electromagnetic disturbances, such as lightning, electrical impulses associated with the switching circuits used in the telephone exchange.

Impulse noise is generally only a minor annoyance for analog data. For example, voice transmission can be corrupted by short clicks and crackles with no loss of intelligibility. However impulse noise is the primary source of error in digital data communication. For example, impulse noise of 0.01 s duration would not destroy any voice data, but would wash out about 50 bits of data is being transmitted at 4800 bps.

1.4 Channel Capacity

The rate at which data can be transmitted over a given Communication Channel, under given conditions, is referred to as the channel capacity. There are four concepts here that we are trying to relate to one another.

• Data rate: This is the rate, in bits per second (bps), at which data can be transmitted.

• Bandwidth: This is the bandwidth of the transmitted signal as constrains by the transmitter and the nature of the transmission medium, expressed by Hertz.

• Noise: The average level of noise over the communications path.

• Error rate: The rate at which errors occur, where an error is the reception of a 1 when a 0 was transmitted or the reception of a 0 when a 1 was transmitted.

Communication facilities are expensive and, in general, the greater the bandwidth of a facility the greater the cost. Furthermore, all transmission channels of any practical interest are of limited bandwidth. The limitations arise from the physical properties of the transmission medium or from deliberate limitations at the transmitter on the bandwidth to prevent interference from other sources. Accordingly, we would like to make as efficient use as possible of a given bandwidth.

Let us consider the case of a channel that is noise-free. In this environment, the limitation on data rate is simply the bandwidth of the signal. A formulation of this limitation, due to Nyquist, states that if the rate of signal transmission is 2W, then a signal with frequencies no greater than W is sufficient to carry the data rate. The conserve is also true: Given a bandwidth of W, the highest signal rate that can be carried is 2W.

However, as signals with more than two levels can be used; that is each signal element can represent more than one bit. For example; if M possible voltage levels are used, than each signal element can represented by $n = \log_2 M$ numbers of bits. With multilevel signaling, the Nyquist formulation becomes

$$C = 2 W \log_2 M \qquad (1.8)$$

Thus, for M = 8, a value used with some modems, C becomes 18600 bps,

An important parameter associated with a channel is a signal-to-noise ratio (SNR) expressed as

$$SNR=10 \log_{10}(S/N) \text{ dB} \qquad (1.9)$$

where S/N - signal -to- noise powers ratio. Clearly a high S/N will mean a high quality signal and a low number of required intermediate repeaters. The signal - to noise ratio is important in the transmission of digital data because it sets the upper bound on the achievable data rate. The maximum channel capacity, in bits per second, obeys the equation attributed as the Shannon - Hartley law

$$C = W\log_2 (1+S/N) \qquad (1.10)$$

2. TELEPHONE AND MOBILE RADIO CHANNELS

2.1 Introduction

A telephone network uses a switching mechanism called circuit switching to establish an end-to-end communication link on a temporary basis. The primary purpose of the network is to ensure that the telephone transmission between a speaker at one end of the link and a listener at the other end is an acceptable substitute for face-to-face conversation. In this form of communication, the mess-sage source is the sound produced by the speaker's voice, and the ultimate destination is the listener's ear. The telephone channel, however, supports only the transmission of electrical signals. Accordingly, appropriate transducers are used at the transmitting and receiving ends of the system. Specifically, a microphone is placed near the speaker's mouth to convert sound waves into an electrical signal, and the electrical signal is converted back into acoustic form by means of a moving-coil receiver placed near the listener's ear. Present-day designs of these two transducers have been perfected so as to respond well to frequencies from 20 to 8000 Hz; moreover, a pair of them is compactly packaged inside a single telephone set that is easy to speak into or listen from. The telephone channel is essentially a linear, bandwidth-limited channel. The restriction on bandwidth arises from the requirement of sharing the channel among a multitude of users at anyone doe. A practical solution to the telephonic communication problem must therefore minimize the channel bandwidth requirement, subject to a satisfactory transmission of human voice. To meet this requirement, the transducers and channel specifications must conform to standards based on subjective tests that are performed on the intelligibility, or articulation, of telephone signals by representative male and female speakers. A speech signal (male or female) is essentially limited to a band from 300 to 3100 Hz in the sense that frequencies outside this band do not contribute much to articulation efficiency. This frequency band may therefore be viewed as a "rough guideline" for the pass band of a telephone channel that provides a satisfactory service.

A great deal of attention has been given to propagation in built-up areas. In particular to the situation where the mobile is located in the streets, i.e. when it is outside the buildings. It is apparent, however, that other important scenarios exist. For example, hand-portable equipment can be taken inside buildings and in (he future, with moves towards a 'personal communications network* (PCN). there is likely to be a substantial increase in the use of this type of equipment. There is therefore a legitimate interest in characterizing the radio communication channel between a base station and a mobile located inside a building. Propagation totally within buildings is also of interest for applications such as cordless telephones, paging, cordless PABX systems and wireless local-area networks. In city areas there are tunnels and underpasses in which radio coverage is needed, and away from cities there arc suburban and rural areas where (lie losses due to buildings are not necessarily the dominant feature.

Before dealing with such channels, however, it is worth pausing to clarify a few points and to identify the ways in which the characteristics of the various channels differ. We wish to distinguish between differences which are merely those of scale and more fundamental differences of statistical character relating to either the signal or the interference. The former category is exemplified by the urban radio channel previously mentioned. This is characterized by Raleigh-plus-lognormal fading and is the same whether the mobile in question is vehicle-borne or hand portable. Differences of scale are apparent because the fading rate experienced by a moving vehicle is, in general, much greater than that apparent to a hand portable. Although these differences do not represent a fundamental change in the statistical nature of the channel, they may not be trivial as far as system designers are concerned. For vehicles moving at a reasonable speed it is often adequate to determine the system performance averaged over the (Raleigh) fading. For a hand portable such a calculation may not be meaningful. In the second category are indoor radio channels where the interference environment differs markedly in magnitude and nature from that outside, and the rural channel where the signal statistics are not well-described by the Raleigh model.

2.2 How a Telephone Works

The telephone is typically located on the customer's premises. It serves as the customer's network access device. Basic parts of the telephone set are:

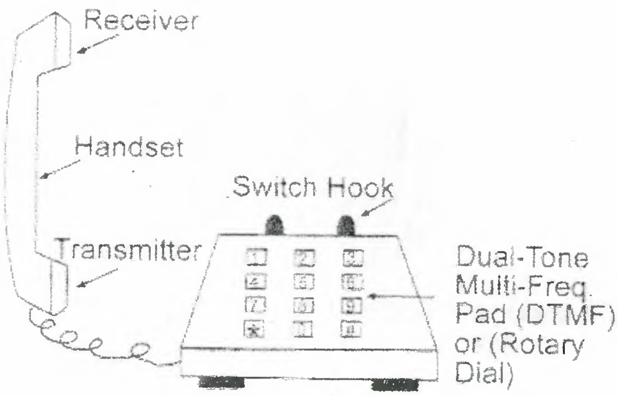

Figure 2.1 Basic parts of the telephone set

a) Ringer

- Always on line

- Alerting device (bell, buzzer) for incoming calls

b) Switch Hook

- Completes the loop (path) when lifted off-hook

Dual-Tone Multi-Frequency Pad (DTMF) or Rotary Dial

- Signaling device that generates the pulses or tone required to identify the called number and billing information

c) Handset

- Contains the transmitter and receiver

d) Transmitter

Converts speech energy (acoustical energy) into electrical energy that can be transmitted over the path to the central office and on to the target destination.

e) Receiver

- Converts the analog electrical signals back into acoustical energy.

The transmitter consists of three parts:

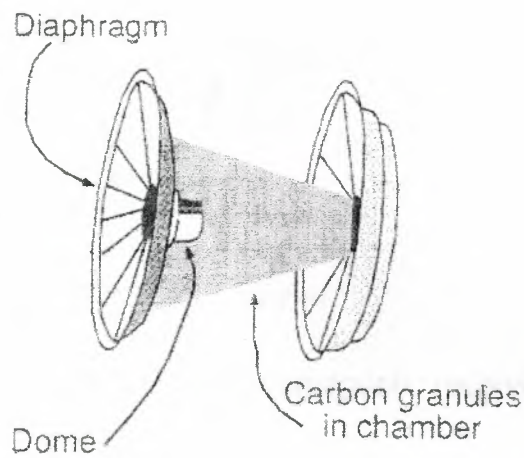

Figure 2.2 The transmitter

1) Diaphragm with a dome
2) Chamber
3) Carbon granules or a conductor

This is how the transmitter works:

Vibrations of the voice sound waves cause the diaphragm to vibrate. The attached dome causes the carbon granules to vibrate (compress or decompress) within the chamber. A current flows from the dome through the carbon granules in the chamber. The amount of current that flows depends on how tightly the carbon granules are packed. Thus, the voice sound wave energy is converted to an electrical energy wave for transmission over the network. The electrical signal is an analogous representation of your voice, hence the term "analog signal."

The most common telephone receiver is the electromagnetic receiver. It also consists of three parts.

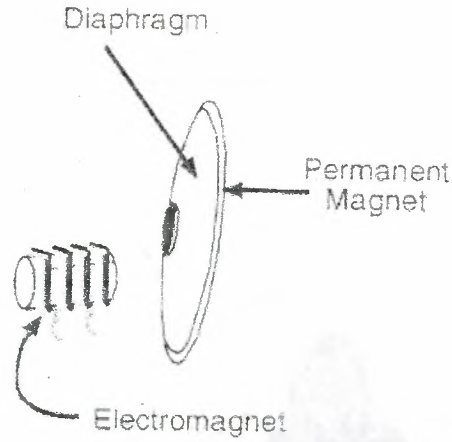

Figure 2.3 The electromagnetic receiver

1) Diaphragm
2) Electromagnetic
3) Permanent magnet

When a varying electrical current flows through the electromagnet, the resulting magnetic field either attracts or opposes the magnetic field of the permanent magnet. This causes the diaphragm to move closer or further away from the permanent magnet (vibrate), in step with the electrical waveform. The electrical waveform is converted back to an acoustical waveform, resulting in a lifelike representation of the original transmission signal. To summarize, the major functions performed by the telephone set are:

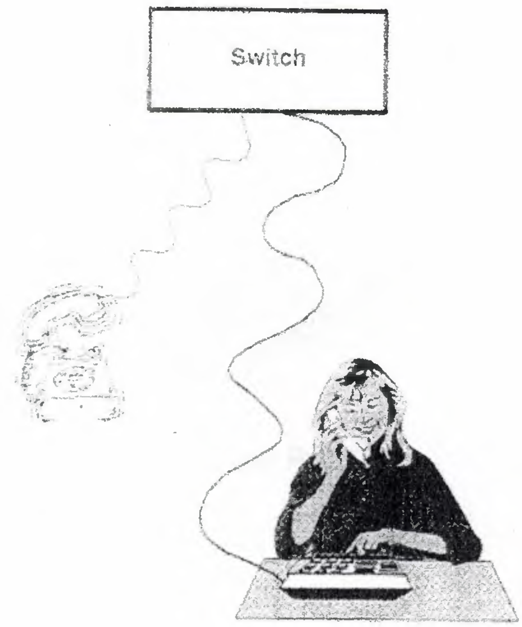

Figure 2.4 Function perform by the telephone set

Requests use of the telephone switching system when the handset is lifted off-hook. Indicates the switching system is ready for use by receiving a dial tone. Generates and sends the telephone number of the address (by dialing the number or by means of a touch-tone keypad).Indicates the status of a call by receiving tones, such as audible ringing, busy tone, or recorded message. Indicates an incoming call by ringing a bell or some other device. Converts acoustical energy into an analogous electrical signal for transmission to a distant party. Converts electrical energy into an analogous acoustical signal representing the sounds of the sender's voice. Informs the system a call is finished when the handset is placed back on the switch hook.

2.3 Telephone Connection to the Central Office

Many customers' telephones are connected to the central office by a pair of wires within a cable. Why two wires?

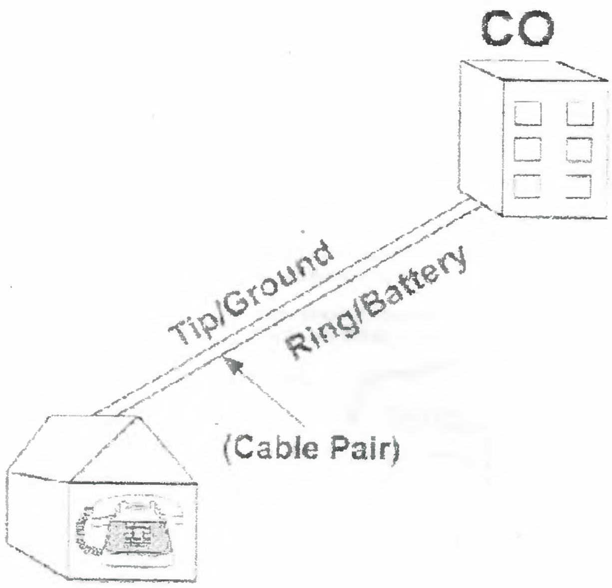

Figure 2.5 Connected to the central

Because your telephone is an electro-mechanical instrument, it requires a battery source and a ground source. The battery source is supplied from the central office equipment to your telephone set by a wire called the ring lead. The ground source is transmitted from the central office by a wire called the tip lead. Together, the tip and ring of the telephone set are commonly referred to as a cable pair.

2.4 Functions of a Switch

The purpose of a switch is to provide a path for the call. To process a call the switch performs three main functions:

2.4.1 Identify the Customers

Initially customers were identified by the jack position they occupied on the switchboard. With the introduction of electromechanical switches, customers were as signed telephone numbers. (Also called line or station numbers.) The customer's cable pair is terminated and cross-connected to the office equipment at the main distributing frame. Office equipment terminated on the MDF represents a physical location in the switch and a specific telephone number. With the introduction of electronic switches, a telephone number is no longer wired to a specific component of the switch. The telephone number is now associated with a customer record which exists in the translations (or memory) of the switch.

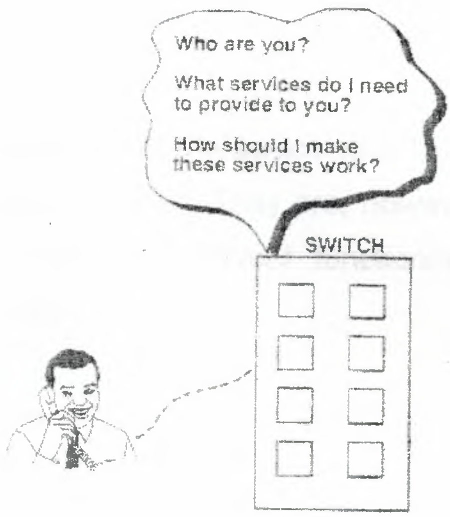

Figure 2.6 Customer records which exists in the translations of the switch

2.4.2 Set up the Path

Early in the processing of a call, the switch needs to determine what type of a call is being made.

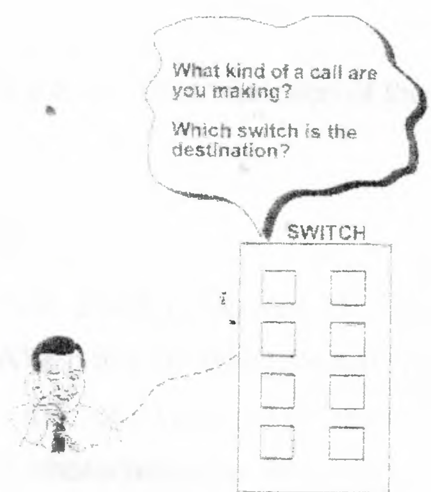

Figure 2.7 Processing of a call

By analyzing either the first digit (is it a 0 or a 1?) or the first three digits (prefix), the switch will determine whether the call is intraswitch or inter-switch. If the call being processed is an intra-switch call, the path that the switch will allocate is called a line (i.e., "on the line side of the network"). If the call is an inter-switch call, the path that the switch will allocate is a trunk.

2.4.3 Supervise the Call

The supervision functions of the switch tend to be overlooked because they are transparent to the customer. They are, however, extremely important because they directly impact the efficient functioning of the switch itself. Supervision functions include:

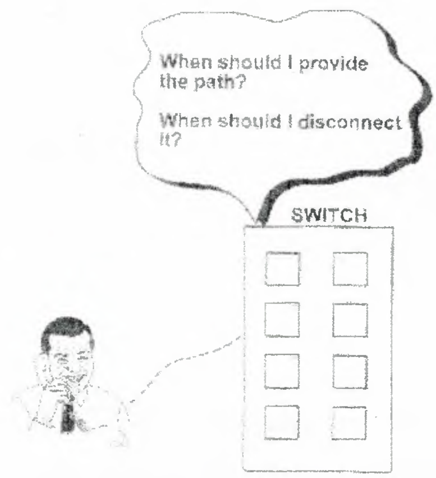

Figure 2.8 Supervision function of the switch

2.5 Digital Switches

Many RBOCs use two primary vendors of digital switches: The #5ESS switch manufactured by AT&T the DMS100 switch manufactured by Northern Telecom Inc. (NTI). At the overview level these switches have similar components and operating characteristics. Illustrates the major components of a 5ESS switch.

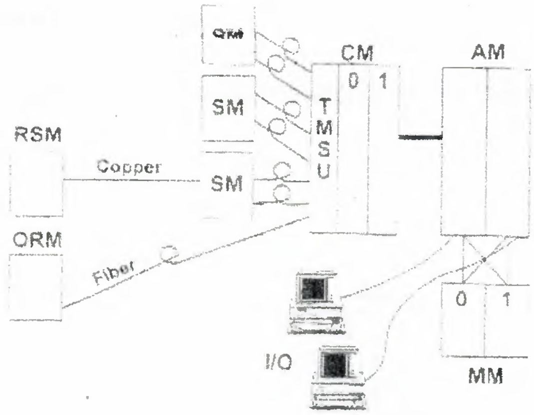

Figure 2.9 Illustrates the major components of a 5ESS switch

- Administration Module (AM)

- Communications Module (CM)

- Remote Switch Module (RSM)

- Switch Module (SM)

- Main Memory (MM)

- Input/Output (I/O)

- Time Multiplex Switch Unit (TMSU) Advantages of digital switches are: - Call processing is executed in nanoseconds (1/1,000,000,000 second)

- A/D & D/A conversion are performed in the SM.

- Digital switches with the appropriate generic (i.e., software or operating system) are required for providing ISDN or remote switch services.

- Digital switches with the proper upgrades are required for AIN

- Digital switches are more efficient in the way they allocate paths through the switch, virtual (time slots vs. physical).

- Digital switches with appropriate hardware/software can reduce D-Banks in the Central Office.

2.6 Administration Module

The three basic pieces of the Administration Module are just like a computer.

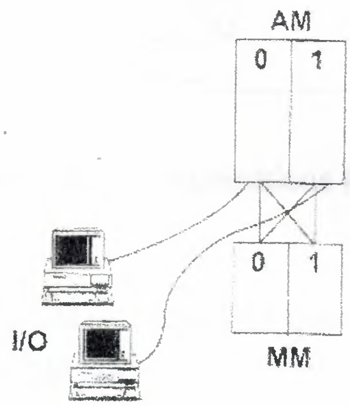

Figure 2.10 The Administration Module

1) Central Processor (CP) Process the stored program from Main Memory to complete call processing for administration functions. There are two 3B20 computers. This provides full duplication of the Central Processor.

2) Main Memory (MM) Storage of call processing programs (Generic program), transient information for administration functions (Parameters and Registers), Line, Trunk and Routing Translations. The Main Memory is fully duplicated.

3) Input/Output (VO) Provides input control to the switch and output to devices that store billing information, maintenance functions, and status information for all equipment within the switch. These are just some of the Input and Output functions.

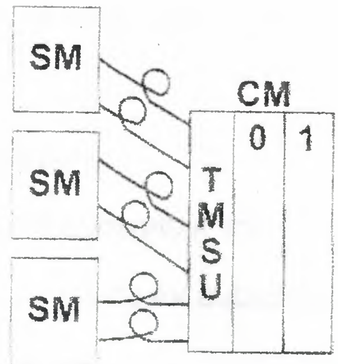

Figure 2.11 Communications Module

The main function of the CM is to interface between the AM and the SMs. Some of the functions of the CM are:

- Switches Subscriber Traffic (Data Time Slots) between SMs. -
- Switches Messages (Control Time Slots) between AM and SMs. -
- Provides System Synchronization. -
- Houses the TMSU. (Time Multiplex Switch Unit)

2.7 Switch Module, Remote Switch Module

The Switch Module (SM) or the Remote Switch Module (RSM) is the connection between the switch and the world. It contains the customer line cards which are connected (wired) to the MDF.

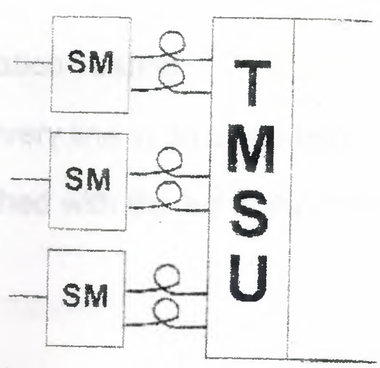

Figure 2.12 The connection between the switch and the world

There are four types of connections:

1) Analog Lines - Customer or subscriber lines.

2) Digital Lines - Digital Data service for subscribers, Subscriber Loop Carriers and ISDN.

3) Analog Trunks - Communications to an Analog switch, or customer's analog switch/PBX.

4) Digital Trunks - Communications path to another Digital switch. Analog switch that has converted the analog signal to a digital signal. A customer's digital switch/PBX.

Switch Modules also have some general functions:

a) Metallic Access

Since a digital switch has eliminated the metallic paths, and only deals in time, there still is a need to test the subscriber's loop (a metallic path) for continuity. The Metallic Access service circuit enables metallic testing for lines or trunks.

b) Transmission Test

Transmission tests are performed on all interoffice trunk groups. These tests ensure that the trunks are at acceptable transmission service levels.

c) Scanner

Device used to monitor lines and trunks to detect OFF-HOOK conditions.

D) Automatic Line Insulation Testing

Automatically tests every line in an office from 2 AM until 6 AM.

These tests are accomplished with the aid of the Metallic Access circuit.

e) Tone Decoder

Detects Multi-Frequency tones on subscriber's lines and trunks.

2.7.1 How the Digital Switch Works

As we saw in the Analog switch, once a call was in a stable condition, that path through the switch could only handle that one call. In a Digital switch, a path in the switch can handle many calls on that one path (fiber link), in fact it can handle about 512 calls on one path. This Fiber Link is called a Network, Control and Timing Links (NCT). The NCT runs from each SM to the CM. The NCT transports the PCM words generated by our A-D or D-A conversion process between the SMs and CM. In addition to the PCM words, it transports Control information needed by either the SM, or the CM. The PCM words are allocated a Time Slot (TS) on the NCT link. So now our path, at least part of our path, has become a time slot on this NCT link. In fact, to complete a call we will need two time slots, one TS for our originating, and one for the terminating.

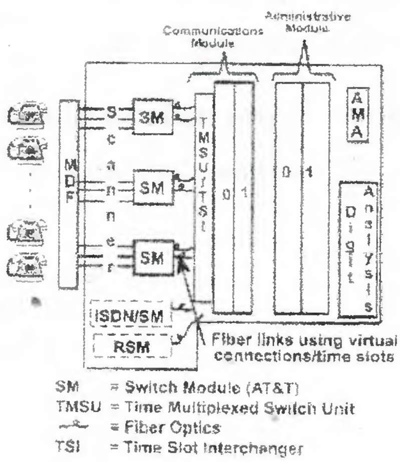

Figure 2.13 A diagrammatic representation of remote modules and the 5ESS

Major Components of a Digital Switch Vendors use different terminology when referring to switch components. Unless stated otherwise, the AT&T terminology will be italicized and the NTI (Northern Telecom Incorporated) terminology will be underlined. Administrative Module (AM) or Central Control Complex (CCC) Communications Module (CM) or Communications Processor (CP) Time Multiplexed Switch Unit (TMSU)

Provides the control functions for the switch; where the software resides along with the decision-making responsibility for the switch; Central Processing Unit (CPU) or main processor are synonyms. Directs traffic through the switch; interfaces with the CPU to collect information required for call processing. Tracks the time slots (moments of time); provides virtual connections between time slots; switches the call. Switch Modules (SM)* or Peripheral Module (PM) Switch interface with the end user; performs the analog to digital and digital to analog conversion. 512 time slots are available between each SM and the TMSU (Time Multiplex Switch Unit) (Line/Trunk translations) Generic or Bulk Change Supplement (BCS) Software that provides control functions for the switch. * Various types of switch modules are: ISDN Switch Modules and Remote Switch Modules.

2.7.2 Remote Switches

Remote switches are a way of providing digital service to customers who would not normally be served from a digital switch. It requires that a digital host (i.e., 5ESS or DMS100) be located within a specified distance of the remote switch. The central processing unit for the remote switch is located at the host.

The SM and CM in the remote location are 95% self-sustainable (in case the host fails) and to process all local calls without the host. The remote switch is connected to a host switch.

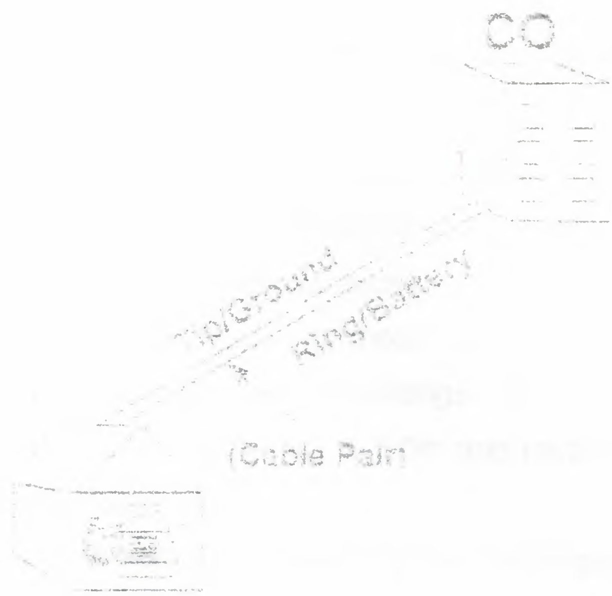

Figure 2.14 Illustrates use of a remote switch

2.8 Building Penetration Losses

As mentioned above, during recent years there has been a marked increase in the use of hand-portable equipment, i.e. transceivers carried by the person rather than installed in a vehicle. Such equipment is particularly useful in cellular and personal radio systems and it is forecast that in the future the number of hand portables will reach the point where they substantially outnumber vehicle-borne installations. For obvious reasons, therefore, it is essential for radio engineers to plan systems that encompass this need and knowledge of the path losses between base stations and transceivers located inside buildings is a vital factor that needs to be evaluated.

The problem of modeling radio wave penetration into buildings differs from the more familiar vehicular case in several respects. In particular.

(1) The problem is three dimensional because at a fixed distance from the base station the mobile can be at a number of heights corresponding to the floor of the building on which it is located. In the urban environment this may result in there being a line of sight path to the floors of many buildings, whereas this is a relatively rare occurrence in city streets.

(2) The local environment within a building consists of" a large number of obstructions. Constructed of a variety of materials. In close proximity to the

mobile, the nature and number of which can change over much shorter distances than in city streets.

There have been several investigations of radio wave penetration into buildings, particularly in the Frequency bands used in cellular systems .these can be divided into two main categories those winch consider the problem for base station antenna heights similar to those used in cellular systems and mobiles operating in multi-storey office buildings. Those that consider base station antenna heights in the range 3.0 to 9.0m and mobiles mainly operating in one or two storey suburban houses.

The investigations in the second category have all originated in connection with the design of a proposed Universal Portable Radio Telephone System. Because such a system would need to cater for large numbers of very low power portables it is based on a very small cell size (< 1.0km radius).Moreover, in such a system it is considered that coverage within multi-storey office buildings will be provided by a number of cells within the building. It is for these reasons that the studies have used low base station antenna heights, base to mobile distances less than 1 km, and have concentrated on taking measurements in buildings the size of suburban houses. In cellular systems, base stations are typically located on the roof of a tall building which may be 100m or more above the local terrain, and base-to-mobile distances greater than 1 km are of interest. Furthermore, the majority of calls might be expected to originate from multi-storey buildings which will not have internal base stations. Consequently, it is difficult to use the results of the above studies in planning cellular systems. However, it is interesting to note that these studies have shown that the signal in small areas within buildings is approximately Raleigh distributed with the scatter of the medians being approximately log normally distributed. In other words the signal statistics within a building can be modeled as superimposed small-scale (Raleigh) and large-scale (lognormal) processes; the model used for radio propagation outside buildings in urban areas. The variation of signal level with antenna height is consistent with the presence of a reflecting ground plane.

With one exception. Studies in the first category referred to above were concerned with the statistical characterization (median or mean, variance. and CPD) of the 'building loss\ a term first introduced by Rice, to denote the difference between the signal on the floor of a building and the median signal level in the streets adjacent to the building. However in reading the literature there is need for some care; this definition has been interpreted in different ways. The method of data analysis also differs, although in almost all investigations the signal has been sampled at fixed intervals of time or distance. In general the different methods of data analysis do not significantly affect the measured value of mean building penetration loss. but calculations of the signal variability can he affected depending upon whether this is described in terms of a standard deviation or as a statistical distribution function.

For these reasons it is difficult to compare the results from the investigations in category above. It is apparent, however, that the penetration loss is dependent on a number of factors including orientation with respect to the base station and the number and size of windows. Moreover, it is clear that other factors such as the height of the transceiver within the building, the propagation conditions along the transmission path and the carrier frequency will play an important role. Almost all models for predicting signal strength in buildings have used the technique proposed by Rice, i.e. firstly predict the median signal level in the neighboring streets using one of the known methods and then add the building penetration loss.

An investigation by Barn and Williamson in New Zealand concentrated originally on buildings where the majority of floors had a line-of-.sight path to the base station. It was found that using criteria similar to those for the vehicular environment, i.e. that the best statistical descriptor was one which adequately predicted values near the tails, the signal on any floor was best fitted by Suzuki statistics. For the experiments, conducted in the 900MHz band, the .standard deviation of the lognormal part of this distribution was 6.7dB. It was also suggested that mirror-glass windows could introduce an additional loss of the order of 10dB.

A series of experiments has been conducted in the UK at frequencies of 441. 900 and 1400 MHz. The general conclusions about signal variability are similar to those from previous investigations but it also proved possible to gain some impression of the effects of transmission conditions and carrier frequency. The transmission conditions appear to have a strong effect on the value of the standard deviation and on the departure of the distribution from lognormal.

frequency is increased from 441 MHz to 896.5 MHz and by a further 4.3dB when the frequency is raised to 1400MHz. These results (the decrease in penetration loss at higher frequency) are consistent with the conclusions drawn by Rice and Mino.

The transmission conditions have a strong influence on the value of the standard deviation and also on the departure of the distribution from log normal. Figure 2.15 shows that when no line-of-sight path exists, the large scale signal variations exactly tit a log-normal distribution and that the standard deviation is about 4dB. In other circumstances where there is a line of-sight path to the whole or part of the building concerned, the large-scale signal variations depart somewhat from the log-normal and have a higher standard deviation. For a complete line-of-sight the standard deviation is lower at 6 7dB. These values are very close to those reported by Cox.

Two building construction effects have been noted. First, the standard deviation of the large-scale variations is related to the floor area of the building concerned, smaller floor areas leading to lower values of standard deviation and vice-versa. Secondly, it has occasionally been found that the penetration loss increases at high levels within a building. A result of this kind was presented without discussion by Walker, where the penetration loss increased from - 1.4dB at floor 9 to 15.3dB at floor 12 of the same building. Although it is difficult to draw a definite conclusion about this finding, it is likely that this increase is related to the relative height of the transmitter and receiver locations, especially when the separation between them is small. This increase will be minimized when the transmitter location is higher than that of the receiver, or where the separation distance is greater. In general, however, the penetration loss reduces as the receiver is moved higher within a building. Figure 2.15 shows a change of about 2dB per floor and this agrees very closely with the findings of other workers.

In summary, when the transmitter is outside, the signal within a building can be characterized as follows:

(!) The small scale signal variation is Raleigh distributed.

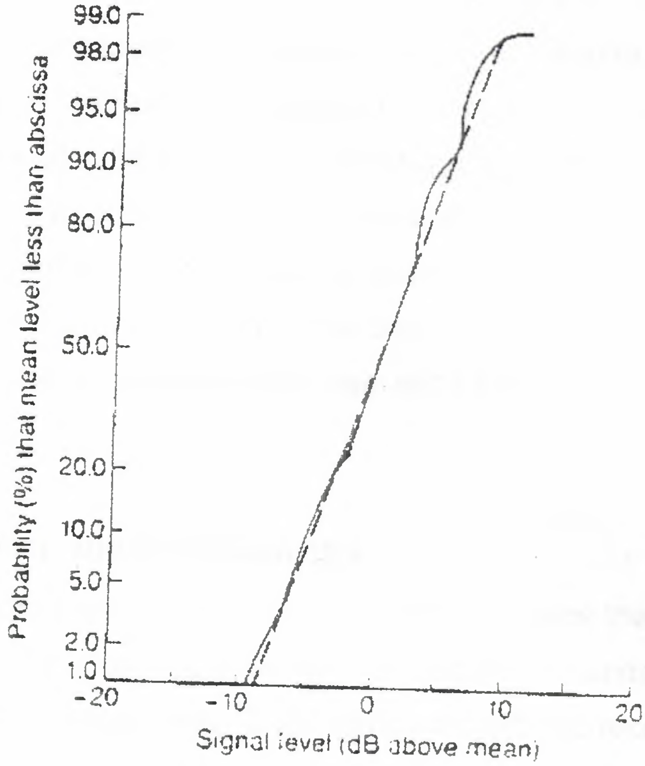

Figure 2.15 Cumulative distributions of the large-scale radiations of the signal at 900 MHz within a building. When no line-of-sight path exists measured

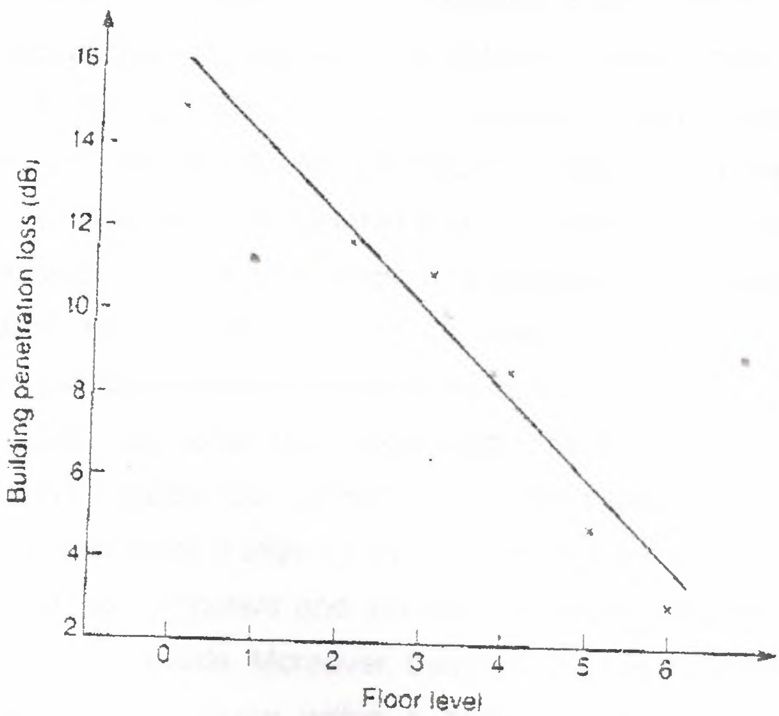

Figure 2.16 Building penetration loss as a function of height within the building

(2) The large scale signal variation is log-normally distributed with a standard deviation related to the condition of transmission and the area of the floor.

(3) The building penetration loss decreases at higher frequencies.

(4) When no line-of-sight path exists between the transmitter and the building concerned (i.e. scattering is the predominant mechanism) the standard deviation of the local mean values is approximately 4dB.When partial or complete line-of-sight conditions exist, the standard deviation rises to 6-9 dB.

(5) The rate of change of penetration loss with height within the building is about 2dB per floor.

2.9 Propagation Inside Buildings

Cordless telephone systems are intended to replace the indoor portion of a subscriber line with a radio link, so that the telephone handset can be carried about freely within a limited area. Calls being initiated and received in the usual way. There is a growing demand for such systems and this demand has prompted research into the propagation characteristics of radio signals within buildings. The possibility of cordless telephone exchanges and the interest in a universal portable radio telephone system arc added factors that have given impetus to this topic. There have been several in vest mat ions over a wide range of frequencies: we will only be able to present rather brief review. However it is worth pointing out at the beginning that propagation within buildings is very strongly influenced by the local features, i.e. the layout of the particular building under consideration and the building construction materials used for the walls, floors and ceilings. It is conceivable, of course, that radio communication inside buildings could be aided by the use of leaky-feeder systems, but that topic will not be considered here.

It was pointed out earlier that indoor radio differs from normal mobile radio in two important aspects; the interference environmental the fading rate. The interference environment is often caused by spurious emissions from electronic equipment such as computers and the level can sometimes be much greater than that measured outside. Moreover, there are substantial variations in signal strength from place to place within a building. The signal can be highly attenuated after propagating a few meters through walls, ceilings and floors or may still be very strong after propagating several hundred meters along a corridor. The signal-to-interference ratio is unpredictable and highly variable. We have already mentioned that the slow fading rate makes it inappropriate to calculate system performance by averaging over the fading; it is more appropriate to envisage two possibilities as follows. First, if the user of a cordless telephone is moving around slowly during the conversation then the antenna will pass through several fades, albeit rather slowly. This situation can best be described in terms of the percentage of time for which the signal-to-interference ratio falls below an acceptable threshold or, in a digital system, the percentage of time for which the error rate exceeds a given value. It is worth pointing out, however, that because of secondary effects (e.g. motion of other people, doors being opened and closed) these probabilities will change slowly with time.

In wideband systems unsatisfactory performance can also be caused by intersymbol interference due to delay spread and this limits the data rate. Thus in narrowband systems, multipath and shadow fading limit the coverage, whilst interference causes major problems even within the intended coverage area. Interference can be natural or man-made noise or can come from other users in a multi-user system. It limits the number of users that can be accommodated within the coverage area. Techniques such as dynamic channel assignment, power control and diversity can be used to reduce the problems.

2.9.1 Propagation characteristics

Several investigations have been undertaken to determine radio propagation characteristics in houses, office buildings and factories. One early investigation, prompted by the proposed introduction of a cordless telephone system in Japan, was concerned with the 250MHz and 400MHz bands. As a result of measurements made using a low-power (10mW) transmitter it was concluded (hat the median path loss follows the free-space law for very short distances (up to 10m) after which it increases almost in proportion to distance. If the propagation path was blocked by furniture of various kinds, the characteristics were affected in different ways and no general statements were made. The short-term variations in signal about the median value were closely represented by a Raleigh distribution as a result of scaling from walls, floors, ceilings and furniture.

The establishment of a law relating path loss to distance from the transmitter is of value in predicting signal strength in a building of a given structure, but it is difficult to make general statements. The best approximations to straight line characteristics arc most likely to occur where rooms are of a similar size. Uniformly arranged, with walls of uniform attenuation between each room. The exponent n in the power law varies from approximately 2 (free-space) along hallways and corridors to nearly 6 over highly cluttered paths.

Motley and Keenan reported the results of experiments in a modern multistory office block at 900 and 1700MHz. A portable transmitter was moved around selected rooms in the building whilst a stationary receiver, located near the centre of the office block, monitored the received signal levels. The conventional power distance law was expressed as

$$P = P + kF = 10n \log_{10} d \tag{2.1}$$

where F represents the attenuation provided by each floor of the building and k is the number of floors traversed. When P' was plotted against distance d, on a logarithmic scale, the experimental points lay very close to a straight line. Table 2.1 summarizes the values of the measured parameters. It can be seen that n is similar at both frequencies but F and S are respectively 6dB and 5dB greater at 1700MHz. These results were confirmed by tests in

Table 2.1 propagation parameters within buildings Frequency

Frequency (MHz)	*F* (dB)	*S* (dB)	*n*
900	10	16	4
1700	16	21	3.5

another multistory building with metal partitioning. Overall, the measured path loss at 1700 MHz was 5.5dB more than at 900 MHz which agrees well with theoretical predictions based on reduced effective antenna aperture.

Similar results have been obtained by other workers who have found that the loss through a double plaster-board wall was 3 to 4dB and through a breeze block or brick wall 7 to SdB. This value is less than that through a floor, probably due to the absence of metal beams and reinforcing meshes which are often present in doors. It seems that at 1650 MHz there is a greater tendency for RF energy to be channeled via stair wells and lift shafts than at 900 MHz.

It appears that propagation totally within buildings is more dependent on building layout and construction in the 1700 MH/ kind than it is at 900 MH/,.The fact that propagation losses increase with frequency is in contrast with observations of building penetration loss where the higher frequencies (end to be advantageous. Nevertheless, it is likely that the 1700MH/ band may be viable for an m-building cordless telephone system where, in any ease. The number of base stations is dictated by capacity and performance requirements rather than by the limitations of signal coverage.

Experiments reported by Bullitude give an indication of signal variability within buildings; it 900 MHZ. Although it might be anticipated that for locations where there is no line-of-sight path, the data would be well represented by a Raleigh distribution as reported .it lower frequencies this did not prove to be the case. Data representing such locations was generally found to be Rican distributed within a secular random power ratio, k, of approximately 2dB. Exceptional locations were found where Raleigh statistics fitted well. For any fixed location having these Rican statistics there is a 90% probability that the signal is greater than -7dB, but less than +4dB with respect to that determined by losses along the transmitter - receiver path. Temporal variations in the received signal envelope are also apparent as a result of movement of people and equipment. These variations are slow and have characteristics that depend upon the floor plan of the building. In buildings which are divided into individual rooms, fading is likely to occur in bursts lasting several seconds with a dynamic range of about 30dB. In open office environments fading is more continuous with a smaller dynamic range, typically 17dB. These temporal envelope variations arc Rican with a value of K between 6 and 12dB. The value of K is a function of the extent to which motion within the building alters the multipath structure near the receiver location.

Terminal motion also causes fading due to movement through the spatially-varying field. This is adequately described as above, by a Rican distribution with k = 2dB.

2.9.2 Wideband measurements

In addition to narrowband measurements designed to determine how median signal strength varies with distance and to evaluate signal variability, there have also been several investigations of the wideband characteristics of propagation within buildings.

Measurements of time delay spread in office buildings and residences have been reported by Devasirvatham using equipment operating at 850MHz with a time delay resolution capability of 25 nanoseconds (i.e., paths differing in length by 7.5m or more can be resolved). It appears that the detailed shape of the individual power delay profiles have little impact on the performance of a radio system so effort was concentrated on presenting the values of the first two central moments, the average delay and the delay spread (root-mean-square delay).

In general the delays and delay spreads are smaller than corresponding values measured outside buildings. The averaged time delay profile in Fig.2.17 represents data collected in a large, six-storey building and has an RMS time delay spread of 247 nanoseconds. Figure 3.4 shows the cumulative distribution of time delay spread for this office building and a smaller two-level building. A portable communications system would have to work under worst-east delay spread conditions which, for both these office buildings, is about 250ns. Larger delay spreads, in (lie range 300 420ns were measured at residential locations particularly on inside-lo-outside paths, but (lie limited number of locations that were used makes general conclusions rather difficult to draw. This interesting work, however, has provided very

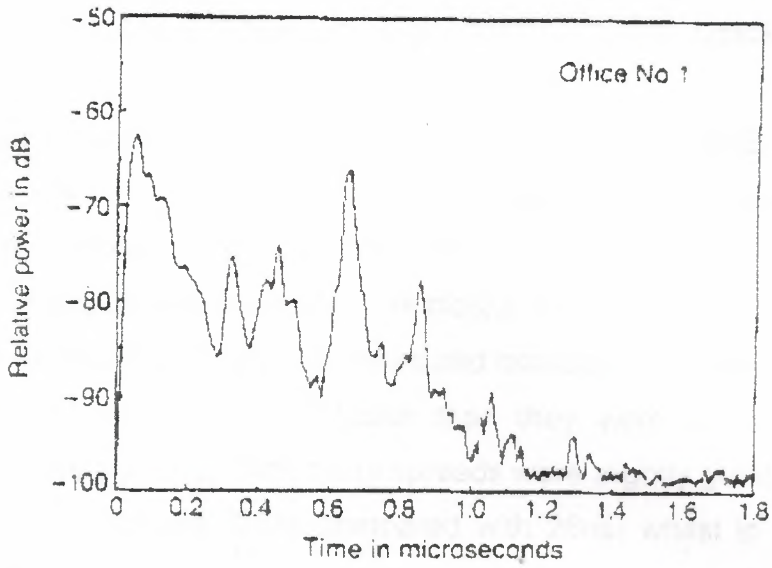

Figure 2.17 Measured time-delay profile within a large six-storey building (After Derasirvatham)

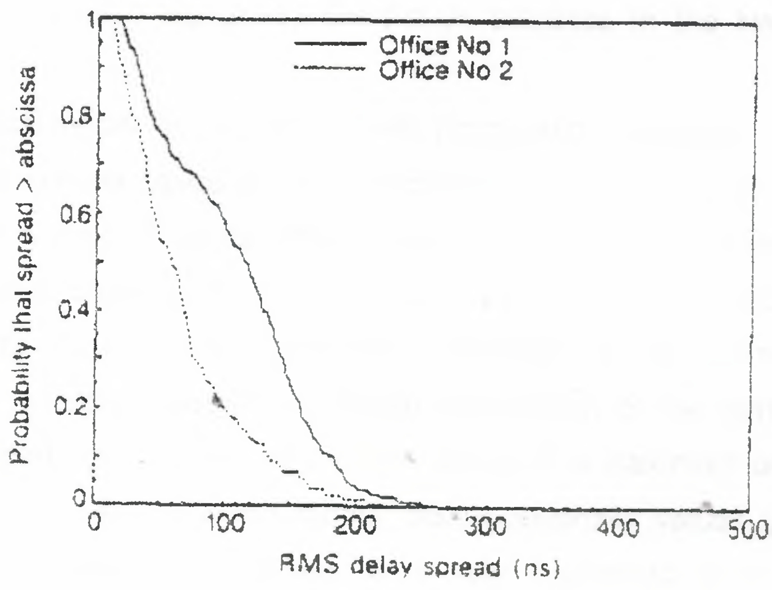

Figure 2.18 Cumulative distribution of time-delay spread within two office buildings

useful data and has demonstrated that in general it is not profitable to attempt synthesis of power-delay profiles from the geometry of the location. It is worth pointing out (hat whenever a line of sight path existed between transmitter and receiver, The RMS delay spread was significantly reduced. typically to less than 100 ns.

Bultilude have compared indoor characteristics at 900 MHZ and 1.75GHZ. Using equipment with parameters the same as that employed by Devasirvatham. Measurements were made in a four-storey brick building and in a modern building of reinforced concrete blocks, both in Ottawa, Canada. There were perceivable differences in the measured characteristics, but these seemed to be more a function of the location than they were of the transmission frequency. In one building, RMS delay spreads were slightly greater at 1.75GHz for over 70% of locations (28ns compared with 26ns) whilst in the other, the reverse was true for about 70% of locations. Whilst the results indicated that coverage would be less uniform in both buildings at 1.75 GHz, they also showed that coverage would be less uniform in one of the buildings than in the other, regardless of the transmission frequency. It seems difficult, on the basis of this work, to conclude anything other than that there is little difference between the wideband frequency correlation statistics in the two frequency bands.

A statistical model for indoor multipath propagation has been presented by Saleh and Valenzuela based on measurements at 1.5 GHz using 10ns radar-like pulses in a medium-sized office building. Their results showed that the indoor channel is quasi-static, i.e. varies very slowly, principally as a result of people moving around. The nature and statistics of the channel impulse response are sensibly independent of the polarization of the transmitter and receiver provided that no line-of-sight path exists. The maximum delay spread observed was 100-200 ns within rooms, but occasionally values greater than 300 ns were measured in hallways. It is very interesting to note that the measured RMS delay spread within rooms had a median value of 25ns and worst-case values of 50ns. These being smaller by a factor of 5 compared with Devasirvatham's results which were obtained in a much larger building. A simple statistical model was proposed in which the rays that make up the received signal arrive in clusters. The ray amplitudes are independent Raleigh random variables with variances that decay exponentially with cluster delay as well as with ray delay within a cluster. The corresponding phase angles are independent random variables uniformly distributed in the range (0.2π). The clusters, and the rays within a cluster, form Poisson arrival processes with different, but fixed, rates and the clusters and the rays have exponentially distributed inter-arrival times. The formation of the clusters is determined by the building structure and the rays within a cluster arc formed by multiple reflections from objects in the vicinity of the transmitter and receiver. Both discrete and continuous versions of the model are possible. More recently, however, it has been suggested that discrepancies arise as a result of the Poisson arrival assumption and that a modified Poisson process is more representative. Furthermore the path amplitudes have been shown to follow a log-normal distribution rather than a Raleigh distribution.

Finally, Rapp port again using similar equipment, have studied multipath propagation in factory buildings at 1300 MHz. Substantial physical differences exist between such buildings and offices or residential houses in respect of construction techniques, contents and placement of walls and partitions. It might be expected, therefore, that propagation characteristics would also be different. In fact it was found that the pall) loss exponent n was approximately 2.2 and that Rican fading was the norm. The RMS delay-spread ranged between 30 and 300ns, the median values being 96 ns for line-of-sight paths along aisles and 105 ns for obstructed paths across aisles. The worst case measured value was 300ns. These values arc comparable with those measured in large office buildings.

Definitive conclusions are not easy because the propagation conditions arc so variable. It seems that where line-of-sight paths exist, the propagation law exponent is usually near 2, indicating that a free-space mode is dominant and this is accompanied by Rican rather than Raleigh fading. For obstructed paths the exponent rises to 4 or more and although in many cases the fading is still characterized by Rican statistics, Raleigh characteristics have also been reported. It is likely that Rican channels will support higher data rates. Wideband measurements have been made at frequencies in the range (S50-1750 MHz but there are no obvious effects that can be attributed to changes in the carrier frequency. There is no evidence to suggest that the scattering and reflecting properties of the materials used for construction, etc. change appreciably over this frequency range, as the delay spreads do not exhibit any significant statistical difference. It might be expected that delay spread would decrease with frequency due to increased attenuation by the structural materials but this is certainly not apparent below 2 GHz. On the other hand, there is some evidence that at 60 GHz the propagation mechanism is different since the radio waves are effectively screened by any metal partitions. Although at this frequency there is some leakage through doors and windows this is insufficient to give room-to-room coupling except where a line of sight path exists. At this frequency the transmission, reflection and absorption properties of materials commonly used for building construction vary very widely. However, no wideband measurements have been reported.

2.10 Radio Propagation in Tunnels

There have been some investigations of radio propagation in tunnels at frequencies of interest for mobile communications. In the VHF band the attenuation is very high and it is only the use of highly directional antennas that makes communication possible within tunnels over distances exceeding a few tens of meters, ft is well-known that a car radio tuned to a normal FM broadcast station loses signal very rapidly when the vehicle enters a tunnel. At higher frequencies there is some improvement although severe problems remain.

Propagation in tunnels is exemplified by an experiment conducted by Reudink in New York. He reports work undertaken in the Lincoln tunnel that connects Manhattan to New Jersey under the Hudson River. The tunnel has a rectangular cross section of dimensions approximately 4m x 7.5m and is about 2425m in length. Propagation tests were made at seven frequencies between 153 MHz and 11.2 GHz using transmitters located within the tunnel, about 300m from the entrance. Figure 7.5 shows some of

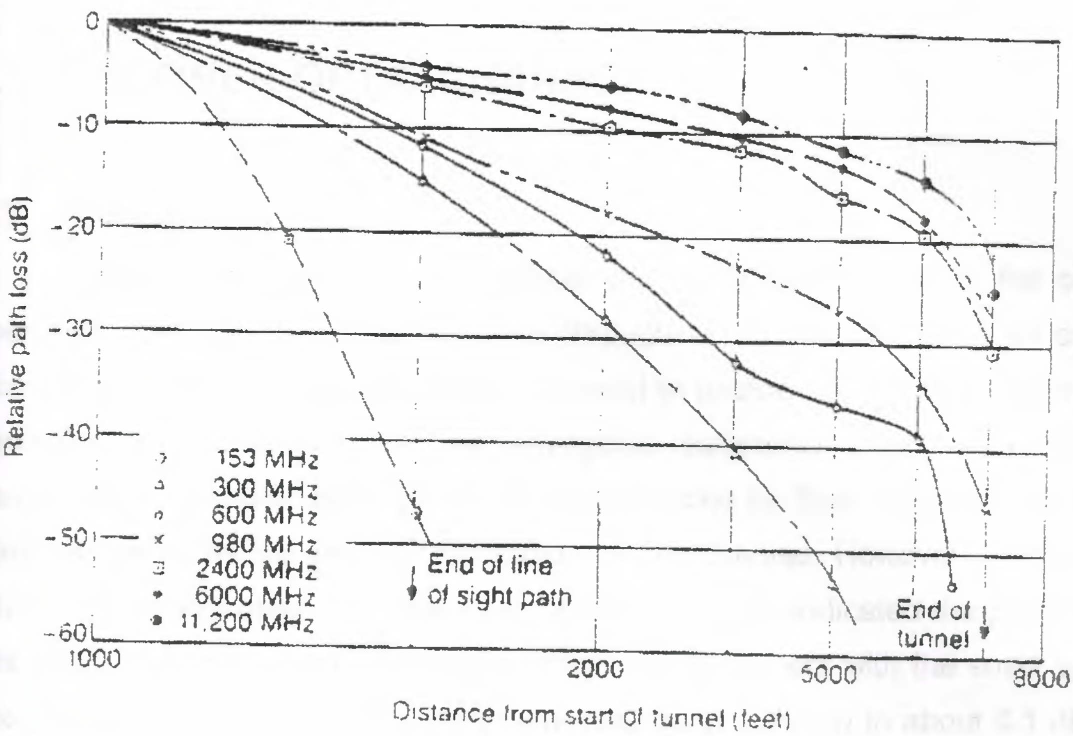

Figure 2.19 Path losses within a tunnel at several different transmission frequencies (after jakes)

the results plotted on a logarithmic scale. It is apparent that attenuation is very high at VHP hut decreases as the frequency is increased. Signal attenuation that follows a .simple d^n law appears as a straight line with a slope that depends on the value of n. Figure 2.19 shows that n is approximately 4 at 900 MHz, reducing to 2 at 2400MHz. Above (his frequency the loss is less than the free-space path loss indicating (lie existence of a guiding mechanism of some kind. At frequencies above 2.4GHz, the attenuation is quite low, making it much more feasible to design a working system. A theory of radio propagation in tunnels has been published. In modern cities it is not uncommon to find an underpass where major roads cross each other. It has been reported that at 900 MHz a 10 to 15dB drop in signal level can be expected in these circumstances and radio communication systems can be severely affected. In general, at frequencies used for the current generation of mobile radio systems propagation problems in tunnels and underpasses are very severe and reliable communication cannot be guaranteed.

3. THE FIBER-OPTIC CHANNEL

3.1 Introduction

Perhaps the most important optical communication channel is the optical fiber. The fiber is a thin "pipe" of glass through which one can shine an optical beam to transmit optical energy from one point to another. The fiber is the optical equivalent of a coaxial cable or waveguide commonly used for microwave transmission. Decades ago attempts to communicate by fiber over long distances were hampered by the severe attenuation of this channel. However, in the early 1970s the demonstration of a fiber with 20dB/km of loss indicated the potential of this link, coupling the high data rates of the optical carriers with the small spatial occupancy of the fiber. Fiber losses have now been reduced to about 0.1 dB/km, and the technological development of solid-state sources and detectors has further advanced the fiber communication channel. In this chapter we attempt to outline the basic communication characteristics of this type of channel.

3.2 The Optical Fiber

The basic construction of an optical fiber. The Core of the fiber is made of high-quality glass over which the light field cans attenuation to the optical transmission. The glass core is supported by a shielding, or cladding, which provides mechanical strength, isolates the core from external interference and radiation, and aids in confining the light propagation to only the internal glass paths. The cladding is opaque, usually constructed of a form of silicon plastic, and attempts to reflect any escaping light back into the core. Typically, the core diameter is on the order of microns, while the fiber cross section (core plus cladding) is on the order of millimeters. Thus the fiber is literally a thread of transmission path over which

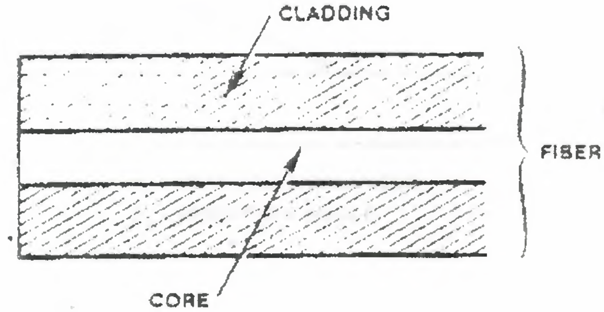

Figure 3.1 Optical fiber construct

the modulated light field can be propagated. The ability to pack large amounts of modulated data over an extremely small spatial area is an overwhelming advantage for optical fiber communications.

As a communication channel, the most important characteristics of the fiber are its attenuation (loss) and its field propagation distortion. The key parameter describing these propagation properties for the fiber core and cladding material is their refractive index. The cladding is designed to have its index slightly smaller than that of the core. (Glass typically has an index of about 1.5, and the cladding index is generally selected to be within a few percent of this value.) Those indices determine the propagation angles of the light rays in the core. The slightly lower cladding index is needed to reflect the off-axis core rays back into the core.

Consider the ray diagram in Figure 3.2 showing an optical ray (optical field propagating in the principal ray direction) being inserted into the fiber core at angle θ_p.If θ_p is too large; the ray will be absorbed into the cladding and will not propagate. Propagation will occur down the fiber only if the incident ray angle at the cladding boundary is shallow enough to be reflected

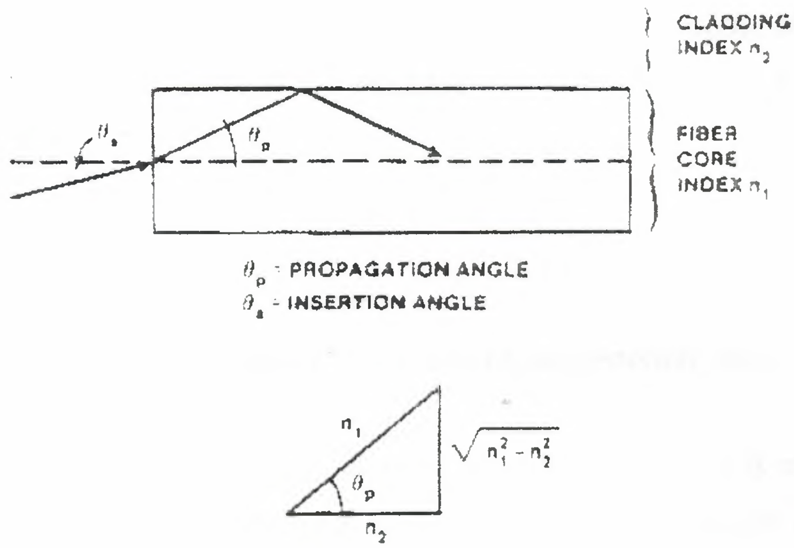

Figure 3.2 Fiber ray diagram

back into the core. The ray will then continue to propagate down the core as it continually reflects off the core walls. The application of Snell's law at the boundary requires that

$$\Theta_p \geq \cos^{1} (n_2/n1) \qquad (3.1)$$

for the reelection to occur, where $n_1$is the core index and n_2 the cladding Index. The right-hand side of Equation (3.1) is called the critical angle of the fiber and represents the maximum ray angle at which light will propagate down the fiber. Note the angle depends only on the index ratio of the cladding and core. By adjusting these indices, one can control these lights flow angles. In particular, by having $n_1 < n_2$ the propagation angles can be made quite small, so the light that propagates does so at small angles (i.e., will How approximately down the center of the core). This means fiber boundary losses will be reduced and less leakage will occur from the core into the cladding. Also, if more than one ray is launched into the fiber simultaneously, each angle must satisfy Equation (3.1), and the various propagating field rays (called fiber modes) all propagate at almost identical angles. Since n: will necessarily be close in value to n_1, we often deal with the fractional difference

$$\Delta = n_1 - n_2 / n_1 \tag{3.2}$$

Of the two indices. For small propagation angles we generally desire a Δ Value of a few percent.

In order to propagate a light ray in the core at angle θ_p, it is necessary that the light field be properly inserted. Let θ_a be the fiber insertion angle; i.e., the angle at which the light is fed into the fiber from an external source, as shown in Figure 3.2. Again, by Snell's law applied to the index change from the fiber external medium (assumed to be free space with index of unity) to the core material, we have

$$n_1 \sin \theta_p = (1) \sin \theta_a = \sin \theta_a \tag{3.3}$$

The numerical aperture of the fiber is defined as

$$NA \, \Delta \sin \theta_a = n_1 \sin \theta_p \tag{3.4}$$

We see that NA is simply an indication of the allowable insertion angle θ_a.For a given core index, we see that a small NA corresponds to a small propagation angle θ_p, and therefore a highly collimated field. Note that Equations (3.1) and (3.4) suggest the triangle relationship in Figure 3.2, And from simple geometry, we see that

$$NA = n_1 \sin \theta_p$$

$$= n_1 (n^2_1 - n^2_2)^{1/2}$$
$$= (n^2_1 - n^2_2)^{1/2}$$
$$= n1 [2(1-n_2/n_1)]^{1/2} \tag{3.5}$$

Thus the numerical aperture is dependent only on the indices $n_1$and n_2. Since $n_1 \approx n_2$we can substitute from Equation (3.2) and use the Approximation

$$NA = n1 [2(1-n_2/n_1)]^{1/2}$$
$$= n^1 (2 \Delta)^{1/2\theta} \tag{3.6}$$

Thus, as an alternative interpretation, when the core index is fixed, NA is actually a measure of the fractional difference of the two indices. Typically, NA takes on values between 0.05 and 0.2.

Our discussion of Figure 3.2 was in terms of a single light ray inserted at angle θ_p. A more typical situation is that shown in Figure 3.3. Here we have a Lambertian light source (light emitted in all directions) shining into the fiber core of diameter d. However, only the light rays with insertion angle θ_a will produce propagating light rays within the critical angle. This

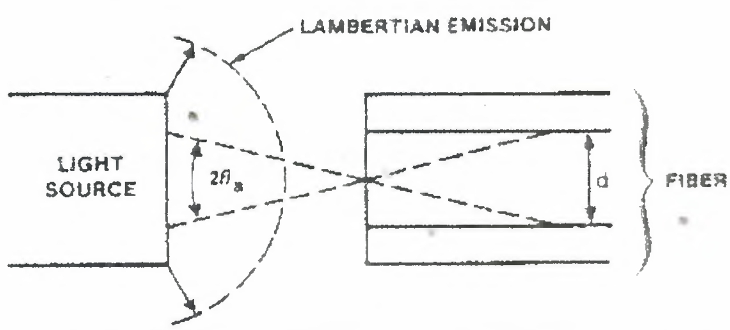

Figure 3.3 Light sources feeding into the fiber

means the fiber only collects the source emissions over the angle 20a. It is therefore natural to define

$$\text{Fiber field of view (sr)} = \pi / 4\,(2\theta a)^2$$
$$= \pi\theta^2_a \qquad (3.7)$$

On the other hand, if we treat the fiber entrance as a collecting area of diameter d for the light at wavelength A, its diffraction-limited field of view (as with any collecting antenna) is then $\lambda^2/\,(\pi d^2/4)$. We can now define the number of received field modes (distinct directions of arrival) per degree of polarization a

$$\text{Number of received field modes} = \pi\theta 2a\,/\,\lambda\,2/\,(\pi d^2/4)$$
$$= \pi^2 d^2\theta^2_a/4\lambda^2$$
$$= \pi^2\,(d/2\lambda)\,2\,(NA)^2 \qquad (3.8)$$

That is, the light from tile external source being collected by the fiber core can be considered to be divided into distinct, independent directions of arrival, each corresponding to a separate diffraction-limited field of view. The number of such modes is given by Equation (3.8). Each such mode, since it corresponds to a proper insertion angle, will produce a separate independent mode (propagating ray line) within the core. Hence Equation (3.8) also gives the number of propagating modes within the core per degree of polarization. For θa » 1, and two degrees of polarization, we therefore have

$$\text{Number of propagating fiber modes} = 2\lambda^2 d^2\theta^2_a/4\lambda^2$$
$$= \tfrac{1}{2}(\pi d^2/\lambda)^2\,(NA)^2 \qquad (3.9)$$

We see for a given NA, which depends only on the fiber indices, the number of propagating modes in the core depends only on the core diameter d. The larger d is, the more modes propagate simultaneously down the fiber. In particular, only one mode will propagate if

$$d \leq (2\lambda)\ 1^{/2}/\pi\ (NA) = 0.45(\lambda/NA) \quad (3.10)$$

Single-mode fibers, therefore, require core diameters to be only several times the optical wavelength.

Mode propagation in a fiber can also be related to the so-called V-number of guided fields. From Maxwell's equations for cylindrical guides, it is known that waves propagate with longitudinal components described in terms of Bessel functions, and the V-number is defined as

$$V = (u^2 + w^2)^{1/2} \quad (3.11)$$

Where

$U = d/2[(2\pi n_1/\lambda)^2 - K^2]^{1/2}$

$W = d/2\ [K^2 - (2\pi n_1/\lambda)^2]^{1/2}$

And k is the longitudinal propagation constant ($K = 2\pi/\lambda$). By direct Substitution we see that

$$V = (\pi d/\lambda)\ [n21 - n^2{}_2]^{1/2} \quad (3.12)$$

Using Equations (3.5) and (3.9) shows that

$$\text{Number of fiber modes} = V^2/2 \quad (3.13)$$

Hence the waveguide V-number is actually a measure of the mode number. Since each mode of the guide corresponds to a zero of a zero-order Bessel Function, single-mode operation requires V be less than the first zero, or

$$V < 2.4 \quad (3.14)$$

Which roughly corresponds to Equation (3.10). We should also point out that

The value of V determines the distribution of the propagating field power between core and cladding. Thus, with V satisfying Equation (3.14), a single
mode will propagate down the fiber, but the actual value of V determines how the power of this mode is distributed radically within the fiber. Figure 3.4 sketches the normalized radial diameter of the single mode as a function of V for V < 2.4. When V is close to 1, the power is widely spread radially and most of the mode power flows in the cladding. As V

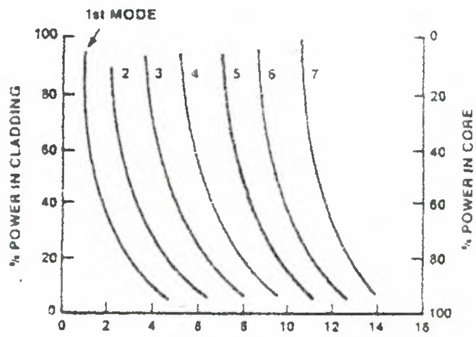

Figure 3.4 Power distributions in core and cladding versus fiber V-number

Increases, more of the power is in the core. For V = 2, about 80% of the field power is in the core. For this case Equation (3.12) requires

$$d = \lambda V / \pi n^{1} (2\Delta)^{1/2} \qquad (3.15)$$

for n_1=1.5 and Δ = 0.003. Tills means a core diameter of several microns must be maintained. When V increases beyond 2.4, new modes are excited and the core power is now redistributed among all modes, as shown in Figure 3.4.

Having V small (V < 1) means that all the power is confined to a single mode and the propagating field is spread significantly into the cladding. This has the advantage of making fiber splicing (connecting two fibers) easier, since exact matching of the cores is not required. However, power flow in the cladding is loosely guided and susceptible to increased attenuation and both leakage and bending losses. Preferred operation is with most of the power in the core, with serious consideration to reducing the V number only in the region of splices. That we can determine the efficiency of coupling into the fiber as

$$\gamma = \iint N(r, \theta) \cos \theta \, d\Omega \, dA, / P_s \tag{3.16}$$

For a point source, y becomes

$$\gamma = \int_0^{\theta a} N(\theta) \cos \theta \, d\Omega / \int_0^{\pi/2} N(\theta) \cos \theta \, d\Omega \tag{3.17}$$

For an isotropic source N (θ) = N for θ defined over a hemisphere, and

$$\gamma = \sin^2 \theta = (NA)^2 \tag{3.18}$$

Hence increasing the NA of a fiber increases the fraction y of source power that will be coupled into the fiber.

3.3 Attenuation and Dispersion in Fibers

In addition to the modal description of a fiber field, one is also interested in the amount of power loss and field dispersion occurring as the field propagates. For a single-mode fiber there is a strong dependence of attenu-ation on wavelength. Figure 3.5 plots the attenuation characteristics of a single mode (dB loss per km) for a glass fiber. This loss is a combination of intrinsic absorption by the atoms which constitute the core and scattering due to core impurities. Absorption loss increases with wavelength, and impurity atoms (iron, chromium, cobalt, copper, etc.) account for the rapid increase in attenuation at the higher wavelengths. Attenuation due to scattering is principally a Raleigh scattering effect and falls off as $1/\lambda^4$, accounting for the increased attenuation at lower wavelengths. This scattering arises from compositional fluctuations which occur of wavelength, and the attenuation coefficient lies somewhere between that predicted by either absorption or scattering alone. Additional losses may have to be included for fiber splicing, cable connections, and fiber bends.

In describing propagating guided fields as a communication channel, one is interested in not only power loss but field dispersion as well. Field dispersion is basically relative displacement of the propagating field components, and leads to waveform distortion in the channel.

There are two main causes of dispersion in a fiber: material dispersion and modal dispersion. Material dispersion is dispersion that occurs within a mode and is caused by the fact (hat the fiber core material causes (he different frequencies that constitute a mode waveform to travel at different velocities within (he mode. Material dispersion is given in terms of time difference in propagating a unit length between two wavelengths AA apart in the vicinity of a wavelength λ. This dispersion is basically proportional to Δ λ and is usually normalized to the percent wavelength difference Δλ/λ.Typical material dispersion is usually stated in nanoseconds per kilometer for a percent bandwidth in wavelengths, as a function of λ for a silicon fiber. The dispersion is about 1 ns/km multiplied by the percent bandwidth at 0.86 μm. An optical bandwidth of about 1000 A would therefore produce about 0.1 ns/km while a 10-A bandwidth produces about 10^{-3}ns/km. Since most microwave modulation formats are in this range, material dispersion of a single mode should have negligible effect on communication performance.

Most dispersion is caused by dispersive interaction between two modes.
Two modes propagating at different ray angles within the core but at the same velocity will arrive at a point down the fiber at different times. Consider the ray diagram in Figure 3.6, showing an outer mode (maximum propagation angle) traveling a different path than the center (θp = 0) mode. While the center mode travels a distance L, the outer mode travels L/cos θp, both

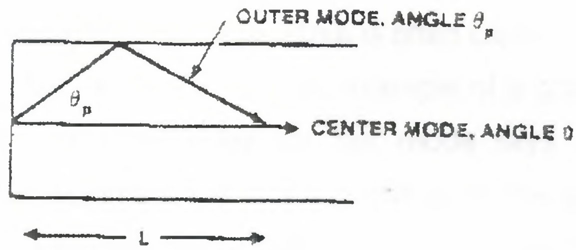

Figure 3.6 Two propagating modes

at the wave velocity c/n_1. The difference between the arrival times of the modes at the plane at L is then

$$t_d = (L/\cos\theta_p - L)\, n_1/c \text{ second} \tag{3.19}$$

Using Equation (3.1) this corresponds to a time differential per unit length of

$$\begin{aligned} T_d/L &= (n_1/n_2 - 1)\, n_1/c = n_1\Delta/2c \\ &= (NA)^2/2n_1c \text{ seconds/length} \end{aligned} \tag{3.20}$$

Hence, worst-case mode dispersion depends only on the fiber indices and varies as the square of the numerical aperture. A fiber with a numerical aperture of 0.2 will have a dispersion of about 50ns/km. That is, light impulses launched at the same time in these two modes will arrive 50 ns apart for each kilometer of fiber.

The derivation of Equation (3.2), using Figure 3.6, immediately suggests that the t_d/L value for these two modes can be decreased by reducing the time differential. This requires speeding up the travel time of the outer ray relative to the inner ray. In order to accomplish this, it is necessary to reduce the core index n_1 at the core edges. Thus the core would have to exhibit a variable index along its radial direction, from n_1 at its center to a decreasing (smaller) value of index grading; this is exhibited as an index profile. Figure 3.7 shows some

graded index profiles. Figure 3.7a is the standard no graded fiber, with the core index n, maintained throughout the core. (This is often called a step-index fiber due to the shape of its profile.) Figure 3.7b is an example of a graded profile, showing the gradual reduction of core index for the mode rays with the increasing propagation angles. In essence, the index profile acts like a continuous tensing action that continually refocuses the light beam along the fiber path.

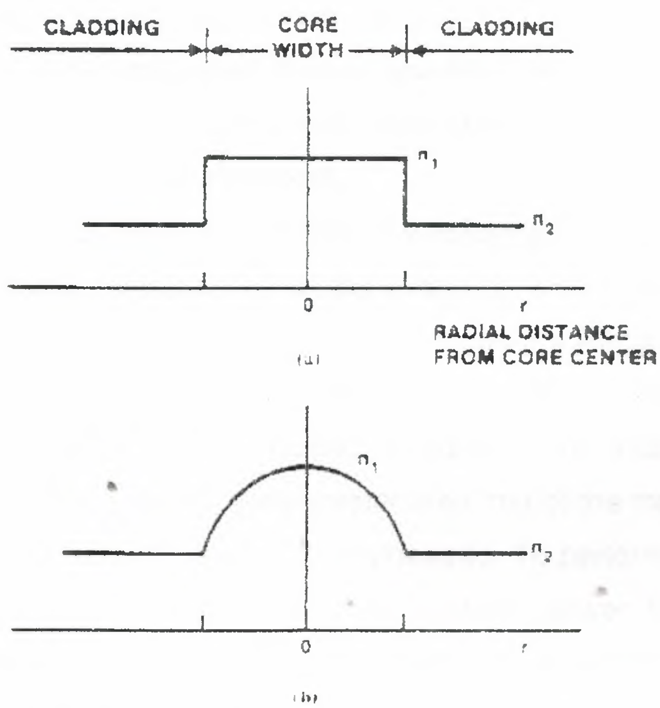

Figure 3.7 Fiber index profile: (a) Step index, (h) parabolic index. A common form of this guiding along the fiber radius r is the parabolic Profile

$$N_1(r) = [1 - q(r/d/2)^2] \quad (3.21)$$

where r is the radial distance from the core center, d is the core diameter, and q is the rate of fiber grading. This profile has a maximum delay spread of approximately

$$t_d/L = (1/\cos\theta)\, n1\ (1 - q)/2c - n_1/2c \quad (3.22)$$

This is about1/Δ times smaller than that for the step-index profile in Equation (3.2). For Δ equal to a fraction of a percent, this corresponds to a reduction in dispersion by several orders of magnitude. Thus, while a standard step-index fiber will have dispersion of about 50ns/km, grade fibers may be well below 1 ns/km. We emphasize that if the single-mode condition can be maintained, mode dispersion does not occur and field dispersion is limited to only that of the core media. The trade-off, of course, is a higher-quality, thinner, low-NA fiber, making splicing and fiber field control more difficult. By using multimode fibers, the latter problems are lessened but the field dispersion is increased.

The use of the previous dispersion analyses employing only central and outer ray lines may raise some questions as to the extent to which this dispersion is really harmful to the propagating field when many modes are involved. With many modes, the field propagates at all ray angles out to the maximum ray angles, and their contribution to dispersion is not included. In addition, the total power of the central (small) angles may be significantly greater than that of the maximum angle, so the effect of the outer angle may be overemphasized. To perform a more exact analysis of field dispersion, it is necessary to consider power flow across all propagating angles and to take into account power conversion that may occur between modes. This is done in the next section.

3.4 Dispersion and Pulse Shaping in Fibers Undergoing Diffusion

A more exact analysis must account for possible power diffusion and mode regeneration as the field propagates. To develop this approach, we must treat the optical Held in the fiber as undergoing diffusion, in which

propagation at one ray direction can couple into another ray angle. This can be handled by considering the ray angle θ as a continuous variable and allowing diffusion over this angle. This inherently implies a multimode condition—a large number of modes existing so that all angles between 0° (central ray angle) and θ_p (maximum ray angle) are occupied.

The modeling of power in a fiber begins with the basic diffusion equation of a propagating field in a medium. In the development here, we follow the illuminating approach of Gloge which is reviewed in Appendix D. We consider the diagram in Figure 3.8 and let

Power in the fiber at time t,

P (, θ, t) Δ (3.23)

Distance z_1 and ray direction θ

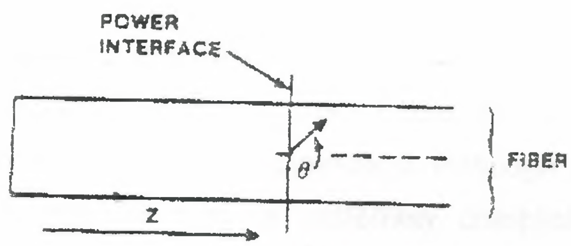

Figure 4.8 Fiber power flow

It is known from diffusion theory that the P function, when confined to small angles 0 as in a fiber, must satisfy the diffusion equation in cylindrical coordinates

$$\partial P/\partial z + (n_1 \cos \theta/c)\ \partial P/\partial t = - A\theta^2 P + 1/\theta\ \partial/\partial\theta\ [\theta D\ \partial P/\partial\theta];\ \theta \ll 1 \quad (3.24)$$

Here c is the speed of light, and A and D are called the attenuation and diffusion coefficients, respectively, of the media. These parameters are determined by the material of the fiber core and are assumed to be constant throughout the core radius.

The total power in the fiber at any time t and position z can be obtained by integrating P over all ray directions. Hence we denote

Integrated power over all ray angles θ
Q (z, t) = at time and position z due to an
initially launched source power distribution

$$= 2\pi \int_{\text{all }\theta} P(z, \theta, t)\ \theta\ d\theta \quad (3.25)$$

Thus Q (z, t) defines the total integrated power that can he collected over the fiber cross-section at a distance; and time /. If the initial source power was an impulse in time [i.e., P (0, θ, t) = 8(t) P0 (θ), where p_0 (θ) is the initiai launch distribution over θ), then Q (z, t) is the impulse response of the fiber at point z.

A complete solution for Q (z, t), from Equations (3.23) and (3.24), was derived by Gloge and is discussed in Appendix 0. Although a completely general solution can be obtained, its form is extremely complicated and somewhat unwieldy to interpret. However, the result has some interesting limiting cases.

For the condition of a "short" fiber, defined by the condition

$$z\gamma_\infty \ll 1 \quad (3.26)$$

the solution reduces to

$$Q(z, t) = (2c/n_1)\ \pi/z\ (1 + z\gamma_\infty)\ e - (2c/n^1\theta^2{}_\infty{}^z)\ t \tag{3.27}$$

The parameter γ_∞ plays the role of an attenuation coefficient (due to both media loss and diffusion), while θ_∞ is like an average diffusion angle, determining the time constant $2c/n^1\theta^2{}_\infty{}^z$ of the exponential decay. Equation (3.35) is plotted in Figure 3.9 for several values of r. Note that as z increases (we move further down the fiber), the peak power decreases, and the impulse response spreads in time according to the time constant Note. That this time constant depends on both the attenuation coefficient A and the diffusion coefficient D of the fiber model.
For a "long" fiber, defined by the condition

$$z\gamma_\infty \ll 1 \tag{3.28}$$

the solution behaves as

$$Q(z, t) = \theta 2\infty\ (\pi/T, t)\ 1/2\ (t/\ z\gamma_\infty T_f + 1/z)\ \exp\{-\ \gamma^2{}_\infty z T_f/4t\} \tag{3.29}$$

$$T_f = n_1/2cA = n_1/2c\ (\theta^2{}_\infty/\ \gamma_\infty) \tag{3.30}$$

Equation (3.38) is included in Figure 3.9 for several values of: $z\gamma_\infty$ .We see that for a long fiber the power response is more pulse like, showing both an inherent delay and a pulse spreading. As the point: is further increased, the pulse delay increases and the shape widens into a wide, bell-shaped

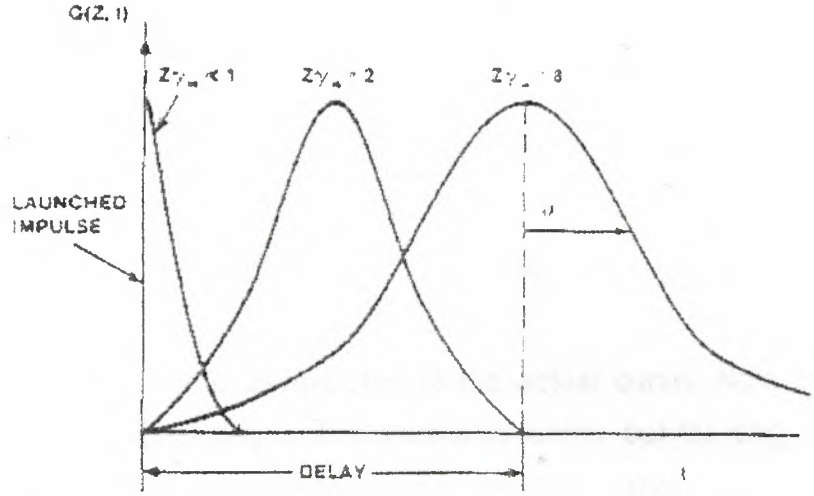

Figure 3.9 Fiber impulse responses in time at various distances in fiber

type of response function. It is convenient to describe these pulse shapes by their "location," or mean delay:

$$\delta(z) = \int_0^\infty tQ(z,t)\,dt \,/ \int_0^\infty tQ(z,t)\,dt \qquad (3.31)$$

and their spread about this delay:

$$\sigma^2(z) = \int_0^\infty [t - \delta(z)]^2\, Q(z,t)\,dt / \int_0^\infty Q(z,t)\,dt \qquad (3.32)$$

Note that Δ is like a "center of mass" of the pulse shape, and σ is like a "variance" about this center. Gloge computed an exact expression for these parameters from his general solution and showed that

$$\sigma^2(z) = T_f/2[\gamma_\infty z\,(1 - 2e^{-\gamma_\infty z}) + \tfrac{1}{4} - e^{-2\gamma_\infty z} + 1/4e^{-4\gamma_\infty z}] \qquad (3.33)$$

The result is plotted in Figure 3.10 as a function of $z\gamma_\infty$, and shows how the power pulse response spreads as it moves further down the fiber.

Equation (3.32) has the limiting forms

$$\sigma^2 (z) = \{(T_f \gamma_,) z \qquad \text{for} \quad z\gamma_\infty \ll 1$$

$$\{(T_f/2) (\gamma_,)^{1/2} \qquad \text{for} \quad z\gamma_\infty \ll 1 \qquad (3.34)$$

which we see are accurate asymptotes to the actual curve. Note that for short distances, the pulse spreading is proportional to length, but for long distances the spreading eventually becomes proportional to the square root

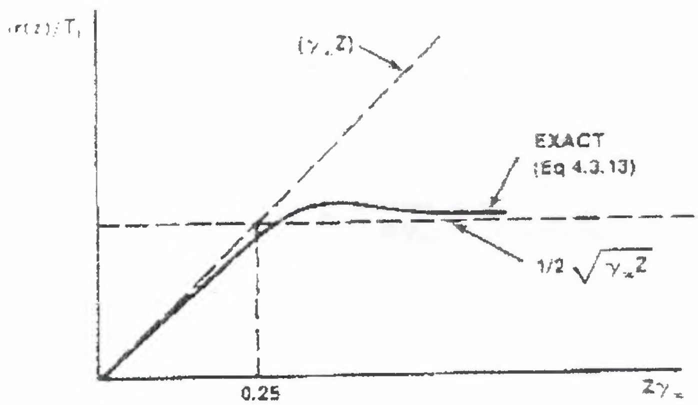

Figure 3.10 Fiber pulse spread σ (z) as a function of distance z in the fiber

of z. That is, the spreading increases at a slower rate at the longer distances. The transition point occurs approximately where the two asymptotes cross, which is at $z\gamma_\infty = 0.25$, or at a distance

$$z_0 \Delta\ 1/4\ \gamma_\infty \qquad (3.35)$$

This is often called the "equilibrium" distance of the fiber. We see from equation (3.34) that this distance z_0 is mathematically related to the attenuation and dispersion coefficients of the fiber core, and therefore depends on the fiber media. On the other hand, since pulse spreading can be readily measured, z_o can be determined empirically. Typically, z_o will have a value on the order of one kilometer for most fibers. A measurement of z_o allows evaluation of the parameter γ_∞ without knowledge of the fiber coefficients.

3.5 Pulse Stretching in Multimode Fibers

The results of the previous section can now be directly applied to model the pulse stretching that occurs in a multimode fiber. Let the fiber length be L and assume a time impulse of power (short burst of light) is launched into the fiber uniformly over all angles less than θ_p. The power distribution, as a function of time, at the fiber output can be obtained by using (he earlier equation with z = L. In particular, the output pulse width will be obtained from (3.33) as

$$\sigma(L) = \begin{cases} T_f \gamma_\infty L & \text{for } L \ll \dfrac{1}{4\gamma_\infty} = z_0 \\ \left(\dfrac{T_f}{2}\right)(\gamma_\infty L)^{1/2} & \text{for } L \gg z_0 \end{cases} \tag{3.36}$$

Furthermore, if we take the average spreading angle θ_∞ to be equal to the maximum propagation angle θ_∞ we can define $T_f \gamma_\infty$ as a fiber spreading coefficient β in seconds/length,

$$\begin{aligned} \beta = T_f \gamma_\infty &= \left(\frac{n_1}{2c}\right)\left(\frac{\theta_\infty^2}{\gamma_\infty}\right)\gamma_\infty \\ &\approx \left(\frac{n_1}{2c}\right)\left(\frac{\text{NA}}{n_1}\right)^2 \\ &= \frac{(\text{NA})^2}{2cn_1} \end{aligned} \tag{3.37}$$

Likewise, we note

$$\frac{T_f}{2}(\gamma_\infty L)^{1/2} = \left(\frac{T_f\gamma_\infty}{2}\right)\left(\frac{L}{\gamma_\infty}\right)^{1/2}$$
$$= \beta\left(\frac{L}{4\gamma_\infty}\right)^{1/2} \qquad (3.38)$$

We can, therefore, write Equation (3.41) directly in terms of β:

$$\sigma(L) = \begin{cases} \beta L & \text{for } L \ll z_0 \\ \beta z_0\left(\dfrac{L}{z_0}\right)^{1/2} & \text{for } L > z_0 \end{cases} \qquad (3.39)$$

Thus, pulse spreading at a fiber output depends on the length of the fiber, its equilibrium distance, and the coefficient β, the latter dependent only on the fiber core index and numerical aperture in Equation (3.36).

Since β determines the amount of pulse spreading that will occur, let us examine it in more detail. If we rewrite the expression for the numerical aperture, we have

$$\beta = n^2_1 - n^2_2/2cn_1$$
$$= n_1 - n_2/c$$
$$= n_1\Delta/c \qquad (3.40)$$

Therefore, the coetlicient β ft depends only on the core index n_1 and index difference A. If we relate this to our earlier result in Equation (3.19), we see that the spreading coefficient β, obtained from diffusion theory, is equivalent to the differential time delay per length t_d/L, obtained from ray line theory. Indeed, the maximum angular ray line contribution to the pulse dispersion is significant, and dispersion reduction via fiber grading is theoretically justified.

3.6 Communications Link Models for the Fiber Channel

The fiber analysis of the previous sections can now be used to formulate a basic fiber optic communication channel model. The procedure is to integrate together the key parameters of the communication link with the channel characteristics of the fiber itself. When viewed in this context, the only role of the fiber is to carry the modulated light field from transmitter to receiver. The characteristics of the channel will therefore depend on the| manner in which the light propagates down the fiber.

A fiber optic communication channel is shown in Figure 3.11. The light! Source emits a modulated optical field, with time-varying power P, (t), into the fiber. The fiber, having length L, is characterized by an attenuation loss factor a (nepers or dB/unit length) and a dispersive effect that is equivalent! To an effective filtering on the light modulation. The field power variation! Collected by the receiver at the fiber output can then be modeled by the^ linear base band filtering

$$P_r(t) = P_t(t) \otimes h_f(t) \tag{3.41}$$

where ® denotes time convolution and h_f (t) is the effective fiber impulses response. For a single-mode fiber, h_f (t) is a wideband response, limited only by the core material dispersion. For a multimode fiber undergoing diffusion, h_f (t) is given by

$$h_f(t) = Q(L, t) \tag{3.42}$$

where Q(z, t) is the response in Equation (3.24) to an optical impulse of power. A direct detection receiver collecting all fiber field modes will produce the photodctected shot noise current, whose mean time variation (signal component) is

$$i_s(t) = \bar{G}a[P_r(t) \otimes h_d(t)] \tag{3.43}$$

where G and u arc photodctcctor gain and responsively, and $h_d(t)$ is the filtering produced by the detector itself on the intensity modulation. In the frequency domain

$$I_s(\omega) = \bar{G}u[\hat{P}_t(\omega)H_d(\omega)H_f(\omega)] \tag{3.44}$$

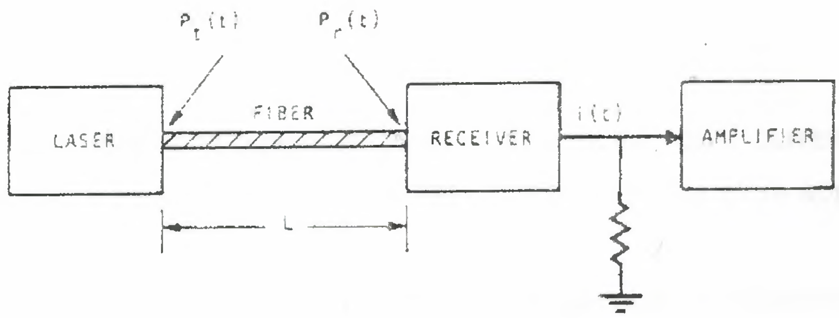

Figure 3.11 Fiber optic communication link

where caps denote Fourier transforms. The conversion of i_s (t) to a signal voltage in Figure 3.11

$$v_s(t) = i_s(t) \otimes h_c(t) \tag{3.45}$$

where $h_c(t)$ is the photo detection filter response corresponding to the transfer function . The resulting detected signal transform is then

$$V_s(\omega) = \bar{G}u[\hat{P}_t(\omega)H_f(\omega)H_d(\omega)H_c(\omega)] \tag{3.46}$$

This establishes the base band equivalent link model shown in Figure 3.12, which describes the way in which light modulation is transmitted to the receiver output. The validity of linear filtering models for optical intensity modulation in fiber systems has been previously investigated. For typical modulation bandwidths, H_d (ω) is relatively wideband, and the principal filtering in Equation (3.44) comes from the fiber and output circuitry.

To the fiber filtering model we can add the photo detector noise, where the noise has spectral level

$$N_0 = \overline{G^2} e\alpha P_r + eI_{dc} + (2kT^\circ / R_L) \tag{3.47}$$

This represents the contribution of detector shot noise, dark current, and post detection thermal noise. The filtered version of this noise therefore appears at the receiver output.

Communication performance for the fiber link can now be determined from the channel model. For example, the detected signal-to-noise ratio (SNR) achievable at the receiver output can be computed by standard power flow analysis. We can first assume the power modulation P_t (t) imposed at the transmitter is narrowband relative to the detector and circuit

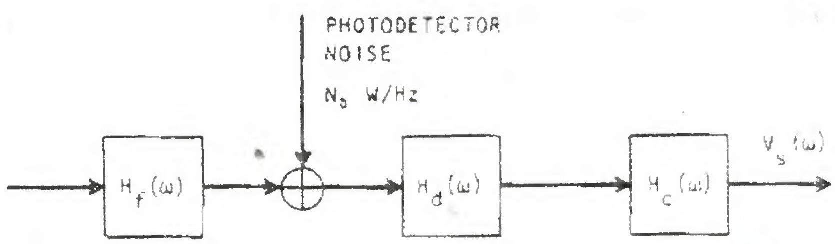

Figure 3.12 Communication model for the fiber channel

filtering. In this case

$$SNR = \frac{(\bar{G}uP_r)^2}{N_0 2B_b}$$

$$= \frac{\left[\left(\frac{\eta}{hf}\right)P_r\right]^2}{\left[\frac{F\eta P_r}{hf} + \frac{I_{dc}}{\bar{G}^2 e} + \frac{2kT^0}{R_L e^2 \bar{G}^2}\right]2B_b} \tag{3.48}$$

with B_b the circuit noise bandwidth P, the average modulation power at the detector input. Solving for Pr gives the required power at the fiber output necessary to establish a desired SNR in a specified bandwidth B_b,

$$P_r = \frac{(SNR)F2B_b hf}{\eta}\left[1 + \left(\frac{2\eta I_{dc}}{hfFeB_b} + \frac{kT^0}{\bar{G}^2 e^2 R_l}\right)\frac{1}{SNR}\right]^{1/2} \tag{3.49}$$

If we introduce the noise-equivalent power (NEP) of the receiver this simplifies Equation (3.59) to

$$P_r = (NEP)[(SNR)2B_b]^{1/2} \tag{3.50}$$

Hence fiber power can be determined from the receiver noise characteristics.

When the receiver is quantum-limited, SNR = ηP_r / $hfF2B_b$, and the required fiber power is simply

$$P_r = (SNR)2B_b Fhf/\eta \tag{3.51}$$

Once the required fiber power is established, the source launch power can be determined from the attenuation. Thus, neglecting fiber dispension,

$$P_t = e^{\alpha L} P_r \tag{3.52}$$

where α is in nepers/length. an overall power analysis to be performed on the fiber channel. Note that with the fiber filtering effect neglected, the analysis is identical to that of a direct detection free-space channel, with background noise neglected, and with fiber attenuation replacing the antenna beam spreading loss.

When fiber filtering is not negligible (i.e., the dispersive effects of the fiber propagation must be included), the degradation in performance due to the resulting distortion on the power modulation P, (r) must be taken into account. In the link model in Figure 3.12, standard Fourier transform theory can be applied to produce the actual time waveform $V_s(t)$, from which distortion effects can be estimated. The use of base band equalizing filters following photo detection to compensate for fiber filtering can be directly applied here.

Of primary concern is when the modulation is transmitted in digital light pulses. The effective channel filtering in Figure 3.12 converts directly to pulse spreading, Pulse distortion of this type, if not carefully designed, can produce degraded digital performance and severely limit data rate capability. This is examined in the next section.

4. THE SATELLITE CHANNEL

4.1 Introduction

Communication between points is achieved by analog or digital modulation of information onto carriers, and by transmission of the carriers as an electromagnetic field from one point to the other. The amount of received carrier power invariably determines the ability of the receiver to demodulate or decode the information. In satellite systems it is extremely important to know the key parameters that directly determine this received power so that proper trade-off in system design between spacecraft and earth stations can be achieved. In this chapter we examine the basic power How equations associated with satellite channels

4.2 Electromagnetic Field Propagation

A basic communication link is shown in Figure 4.1. The transmitter field is characterized by its effective isotropic radiated power (EIRP) defined by

$$\mathrm{EIRP} = P_T g_t(\phi_z, \phi_l) \tag{4.1}$$

where P-r is the available antenna input carrier power from the transmitter power amplifier, including circuit coupling losses and antenna radiation losses, and $g_r(\Phi z,\Phi l)$ is the transmitting antenna gain function in the

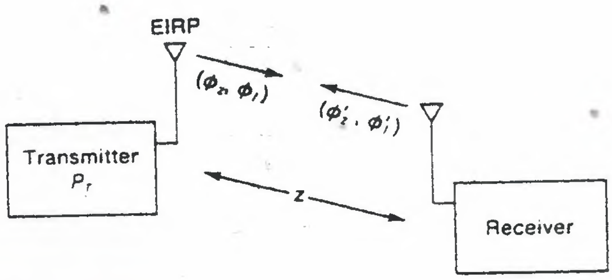

Figure 4.1 Communication link

angular direction (Φz,Φl) of the receiver. Here (Φz, Φl) refer to azimuth and elevation angle, respectively, measured from a coordinate system centered at the transmitting antenna. The flux density or field intensity of the electromagnetic field at the receiver due to the transmitter field is then

$$I\,(z) = (EIRP)\ L_a/4\pi z^2 \tag{4.2}$$

where : is the propagation distance to the receiver and Ly accounts for the atmospheric losses during propagation. The received carrier power collected by the receiving antenna having area A_r normal to the direction of the transmitter is then

$$P_r\ = I\,(z)\ A_r = (EIRP)\ L_a/4\pi z^2 \tag{4.3}$$

The receiving area A_r can be written in terms of the receiving antenna gain function g_r in the direction of the transmitter:

$$A_r = (\lambda\,2/4\pi)g_r(\Phi'z,\Phi'l) \tag{4.4}$$

where a is the carrier wavelength and (Φ'z,Φ'l) are the azimuth and elevation angles of the transmitter relative to the receiver coordinate system. Combining this equation with Eq. (4.3) allows us to rewrite

$$P_r = (EIRP)\ LaL_pg_r\ (\Phi'z,\Phi'l) \tag{4.5}$$

where we have defined

$$L_p = \left(\frac{\lambda}{4\pi z}\right)^2 \tag{4.6}$$

The parameter Lp appears as an effective loss occurring during transmission and is referred to as the propagation loss of the link. Note that Lp depends on both the carrier frequency through the wavelength A and on the distance r, and its loss is always present, even if there are no atmospheric losses (i.e., if there is free space transmission outside the Earth's atmosphere). We often state P, in terms of decibels, and write

$$(P_r)_{dB} = (\mathrm{EIRP})_{dB} + (L_p)_{dB} - (L_a)_{dB} + (g_r)_{dB} \tag{4.7}$$

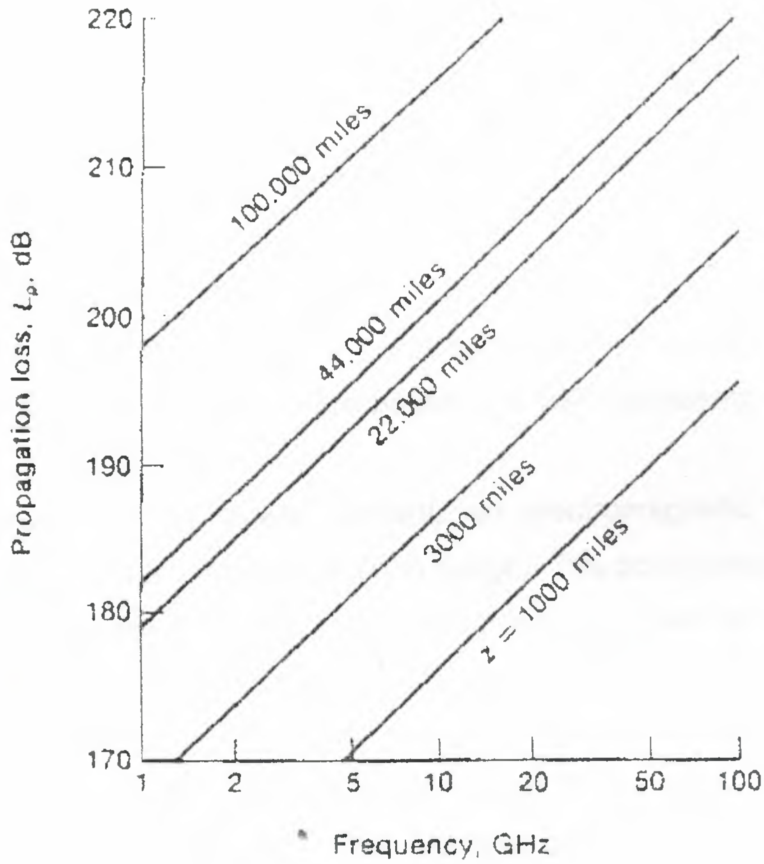

Figure 4.2 Satellite propagation losses

where each term is computed in decibels. Note that gain values (greater than 1) are always positive (add) decibels; whereas attenuation losses (less than 1) are always negative (subtract) decibels. The propagation loss, L_p, when converted to frequency has the decibel value

$$(L_p)_{db} = -36.6 - 20 \log_{10} [z \text{ (miles) } f \text{ (MHZ)}] \tag{4.8}$$

A plot of $(L_p)_{db}$ for typical satellite distances and satellite frequencies is shown in Figure 4.2. Note that about several hundred decibels of propagation loss will generally occur in satellite communication paths for geostationary orbits. The exact value depends on the actual satellite slant range to the earth station; another parameter often specified in satellite link analysis is the received isotropic power (RIP). This is obtained from Eq. (4.5) as

$$RIP = (EIRP)\, L_a L_p \tag{4.9}$$

or in decibels as

$$(RIP) = (EIRP)_{db} + (LaLp)_{db} \qquad (4,\ 10)$$

The RIP represents the transmitted power that would be collected by the receiver antenna if it were ideally isotropic. Thus, Whereas EIRP indicates the ability of a transmitter to radiate power; the RIP represents the available field power at the receiver.

In addition to its power content, an electromagnetic field also has a designated polarization (orientation in space). Tills polarization is determined by the manner in which the electromagnetic field is excited at the antenna feeds prior to propagation. An additional receiver power loss will occur if the receiving antenna subsystem is not properly aligned with the received wave polarization. This is referred to as a polarization loss, and should be included in the L_p loss term in Eqs. (4.2) and (4.7). The common polarizations in satellite links are linear and circular. In linear polarization the electromagnetic field is aligned in one planar direction throughout the entire propagation, as shown in Figure 4.3a. These directions are usually designated as horizontal or vertical polarizations (relative to the receiving antenna coordinates). The receiving antenna system must have a matching planar receptor in order to maximize the collected power. For example, terrestrial commercial television is transmitted as a horizontally polarized field, and our rooftop antennas utilize

horizontal dipole rods for reception. In circular polarization (CP) the field is excited and transmitted with

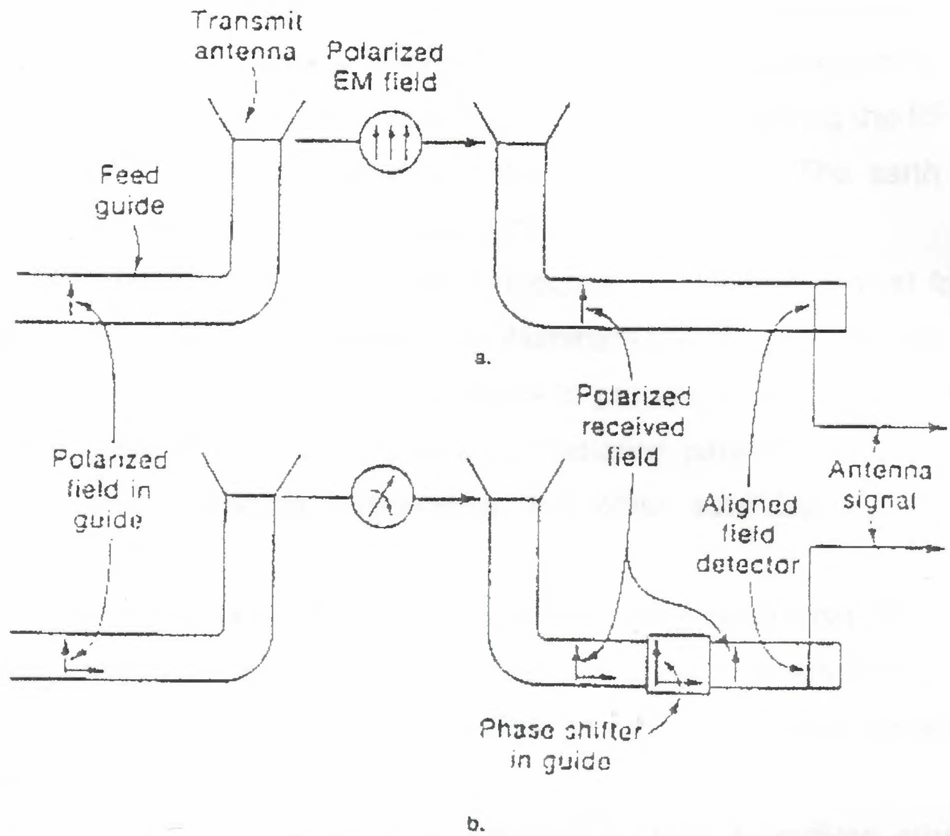

Figure 4.3 Transmitted and detected field polarizations: (a) linear: (b) Circular

components in two orthogonal coordinates (one horizontal and one vertical) dial are phased so that the combination of the two produces a resultant field polarization that appears to rotate circularly as the wave propagates (Figure 4.3b). CP reception is achieved by an antenna that feeds both components into an antenna waveguide and that uses internal phase shifters to reorient one orthogonal polarization onto the other, there by collecting the total power available in both components. CP has the advantage that any extraneous rotation of the polarization axis caused by the atmosphere will not affect CP reception, whereas such rotation will produce a polarization loss in a linearly polarized system.

4.3 Antennas

The earth station antenna is one of the important subsystems of the RF terminal because it provides a means of transmitting the modulated RF carrier to the satellite within the uplink frequency spectrum and receiving the RF carrier from the satellite within the downlink frequency spectrum. The earth station antenna must meet three basic requirements:

1. The antenna must have a highly directive gain; that is, it must focus its radiated energy into a narrow beam that illuminate the satellite antenna in both the transmit and receive modes, and hence to provide the required uplink and downlink carder power. Also, the antenna radiation pattern must have a low side lobe level to reduce interference into other satellites and terrestrial systems.

2. The antenna must have a low noise temperature so that the effective noise temperature of the receive side of the earth station, which is proportional to the antenna temperature, can be kept low to reduce the noise power within the downlink carder bandwidth.

3. The antenna must be easily steered so that a tracking system (if required) can be employed to point the antenna beam accurately toward the satellite taking into account the satellite's different in position. This is essential for minimizing antenna-pointing loss.

4.3.1 Antenna Types

The two most popular earth station antennas that meet the above requirements are the parabolic antenna with a focal point feed and the Cassegrain antenna. A parabolic antenna with a focal point feed is shown in Figure 4.4. This type of antenna consists of a reflector, which is a section of a surface formed by rotating a parabola about its axis, and a feed whose phase centre is located at the focal point of the parabolic reflector. The size of the antenna is represented by the diameter D of the reflector. The feed is connected to a high power amplifier and a low noise amplifier through an orthogonal mode transducer (OMT) which is three port networks. This type of antenna is easily steered and offers reasonable gain efficiency in the range of 50 to

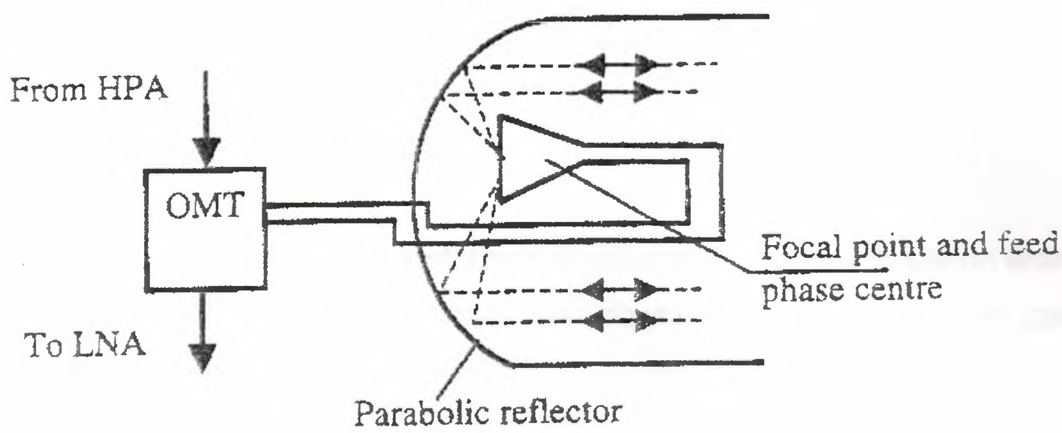

Figure 4.4 A parabolic antenna with a focal point feed

0%. The disadvantage occurs when the antenna points to the satellite at a high elevation angle. In this use, the feed radiation which spills over the edge of the reflector illuminates the ground whose noise 'mperature can be as high as 290° K and results in a high antenna noise contdbution.A Cassegrain antenna is a dual-reflector antenna, which consists of a main reflector whose focal point is coincident with the virtual focal point of a hyperboloid sub reflector in Figure 4.6. On the transmit side, the signal energy from the output of the high-power amplifier is radiated at the real focal point by the feed and illuminates the convex surface of the sub reflector which reflects the signal energy back as if it were incident from a feed whose phase centre is located at the common focal point of the main reflector and sub reflector. The reflected energy is reflected again by the main reflector to form the antenna beam.

On the receive side, the signal energy captured by the main reflector is directed toward its focal point. However the sub reflector reflects the signal energy back to its real focal point where the phase center of the feed is located. The feed therefore receives the incoming energy and routes it to the input of the low-noise amplifier through the OMT. A Cassegrain antenna is more expensive than a parabolic antenna because of the addition of the sub reflector and the integration of the three antenna elements - the main reflector, sub reflector, and feed - to produce an optimum antenna system.

However, the Cassegrain antenna offers many advantages over the parabolic antenna: low noise temperature, pointing accuracy, and flexibility in feed design.

Since the spillover energy from the feed is directed toward the sky whose noise temperature is typically less than 30K.

4.3.2 Parameters of antenna

a) Antenna Gain

Gain is perhaps the key performance parameter of an earth station antenna because it directly affects the uplink and downlink carrier power. The gain is given by

$$G = \eta(\pi fd/c) \tag{4.11}$$

where

D - antenna diameter (m).

f - radiation frequency (Hz)

c - speed of light = 2.997925 10

m/st|- antenna aperture

efficiency (%0.95)

b) Antenna Pointing Loss

A loss in gain can occur if the antenna-pointing vector is not in line with the satellite position vector a shown in Figure 4.5. The antenna pointing loss can be evaluated from the antenna gain pattern, which is a function of the off-axis angle.

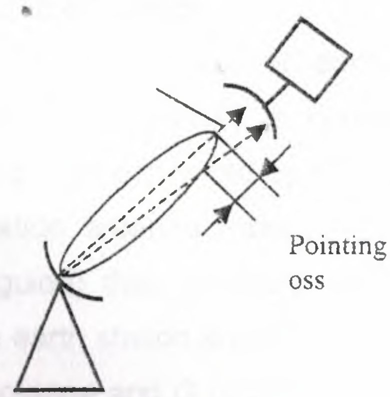

Figure 4.5 Antenna pointing vector

Because the earth station antenna is subjected to a wind loading effect and the satellite drifts in orbit, an antenna tracking system is necessary for a large diameter antenna to minimize the pointing error. The antenna tracking system is a closed-loop pointing system; that is, the antenna-pointing vector, which is function of the azimuth and elevation angles, is derived from the received signal. One

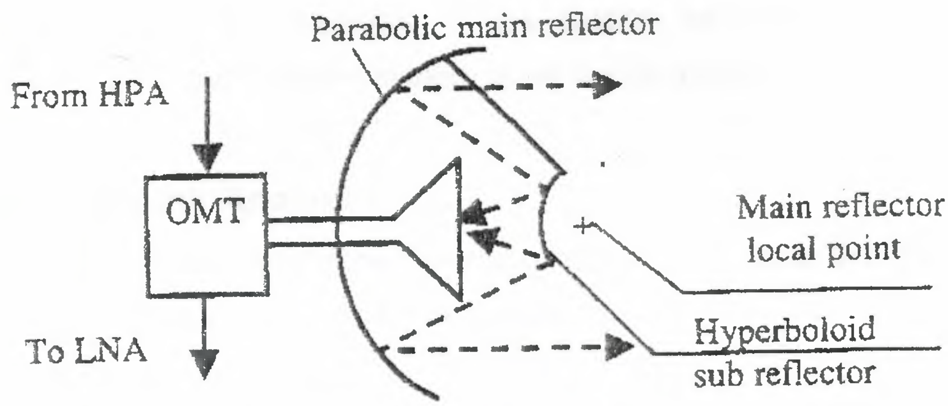

Figure 4.6 A parabolic antenna with a Main reflector local point

of the commonly used antenna tracking systems for earth stations is a step track which derives the antenna pointing vector from the signal strength of a satellite beacon.

c) Effective Isotropic Radiated Power

To express the transmitted power of an earth station or a satellite, the effective isotropic radiated power (EIRP) is normally employed. The earth station EIRP is simply the power generated by the high –power amplifier times the gain of the earth station antenna, taking into account the loss in the transmission line (wave guide) that connects the output of the high power amplifier to the feed of the earth station antenna. If we let P (t) denote the input power at the feed of the antenna and G (t) the transmit antenna gain, the earth station EIRP is simply

$$EIRP = P(t) \cdot G(t) \quad (4.12)$$

d) Antenna Gain-to-Noise Temperature Ratio

The antenna gain-to-noise temperature ratio G/T is a figure of merit commonly used to indicate the performance of the earth station antenna and the low-noise amplifier in relation to sensitivity in receiving the downlink carrier from the satellite. If a piece of waveguide with a 0.53-dB loss is used to connect the input of the low noise amplifier to the output port of the feed system, the receive antenna gain referred to the input of the low noise amplifier is simply 65 dB. The parameter T is defined as the earth station system noise temperature referred also to the input of the low-noise amplifier. We have discussed the antenna gain previously, therefore in this section we will concentrate on determination of the earth station system noise temperature.

4.4 Satellite Link Analysis

The CNR link budgets of the preceding section can now be directly applied to the analysis of specific satellite links.

4.4.1 Satellite Uplink

Figure 4.7 sketches a simplified earth-station-satellite uplink. Transmitter power for earth stations is generally provided by high-powered amplifiers, such as TWTs and klystrons. Since the amplifier and transmitting antenna are located on the ground, size and weight are not prime considerations, and fairly high transmitter EIRP levels can be achieved.

Earth-based power outputs of 40-60 dBw are readily available at frequency bands up through K-band, using cavity-coupled TWTA or kly- strons (Angelakos and Everhart, 1968). These power levels, together with the transmitting antenna gains, determine the available EIRP for uplink communications.

In the design of satellite uplinks, the beam pattern may often be of more concern than the actual uplink EIRP. Whereas the latter determines the power to the desired satellite, the shape of the pattern determines the amount of off-axis (side lobe) interference power impinging on nearby

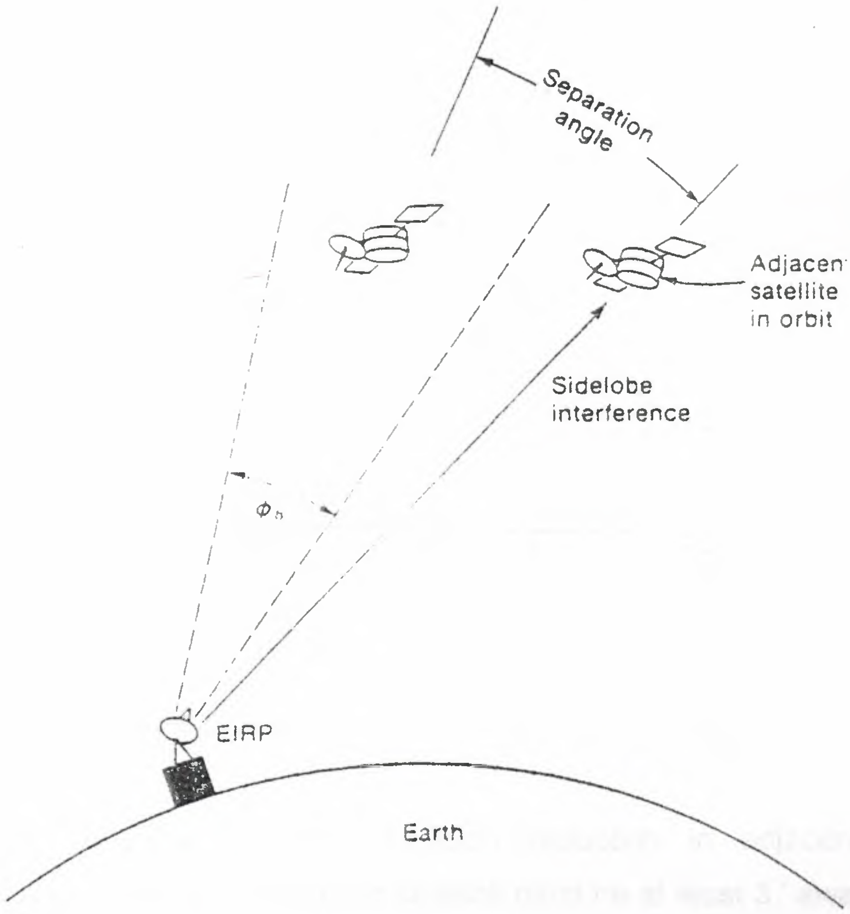

Figure 4.7 Satellite uplink

satellites. The beam pattern therefore establishes acceptable satellite spacing, and thus the number of satellites that can simultaneously be placed in a given orbit with a specified amount of communication interference. The narrower the earth-station beam, the closer an adjacent satellite can be placed without receiving significant interference. On the other hand, an extremely narrow beam may incur significant pointing losses due to uncertainties in exact satellite location. For example, if a satellite location is known only to within ±0.2°, a minimum earth-station half-power beam width of about 0.6° is necessary. This sets the transmit antenna gain at about 55 dB, this produces the off-axis gain

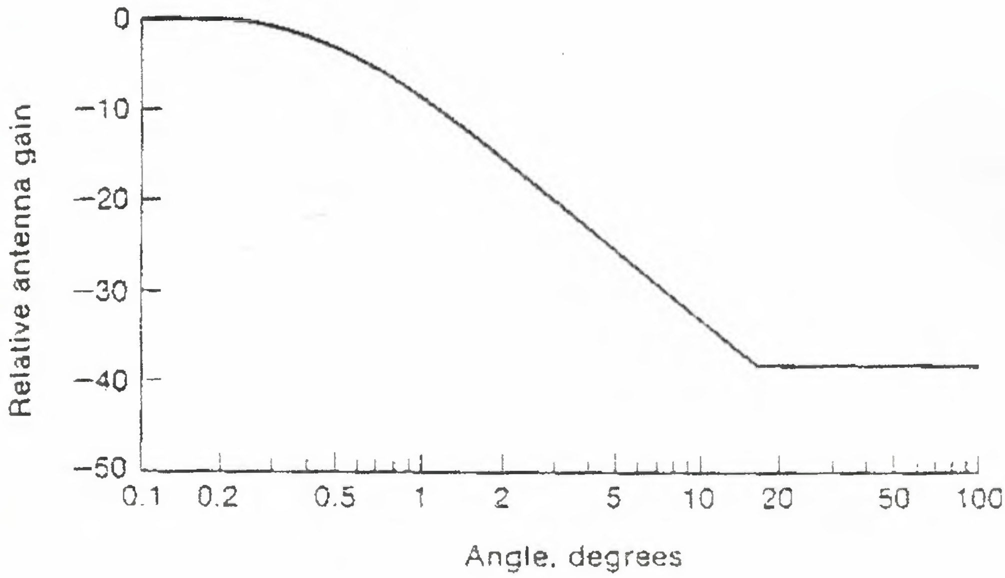

Figure 4.8 Uplink earth-station antenna pattern. Angle measured from boresight

curve shown in Figure 4.8.For a 20dB reduction in adjacent satellite interference, we see that the nearest satellite must he at least 3 ' away. That is, when observed from earth. Two satellites in the same orbit must be separated by about 3 in Figure 4.7. Thus, the uplink beam width is set by the pointing accuracy of the earth station, whereas satellite orbit separation is determined by the acceptable side lobe interference. If satellite pointing is improved, the uplink beam width can be narrowed, allowing closer satellite spacing in the same orbit. This would increase the total number of satellites placed in a common orbit, such as the synchronous orbit.

With the half-power beam width set, a higher carrier frequency will permit smaller earth stations. Figure 4.9 shows the relation between earth-station antenna diameter and frequency in producing a given uplink beam width and gain, using Eqs. (4.13) and (4.14). Note that while increase of carrier frequency does not directly aid receiver power, we see that an advantage does accrue in reducing earth-station size and, possibly, in improving satellite trafficking (allowing more satellites in orbit).

With a 0.6° uplink beam width (gain ≈ 55 dB) earth-station EIRP values of about 80-90 dBw are readily available. An example uplink budget for computing the CNR at the satellite in a 10-MHz bandwidth, showing the way in which the entries of Eq. (4.15) are individually computed and combined. Figure 4.9

generalizes this budget to show how CNR will vary with earth-station EIRP and satellite receiver

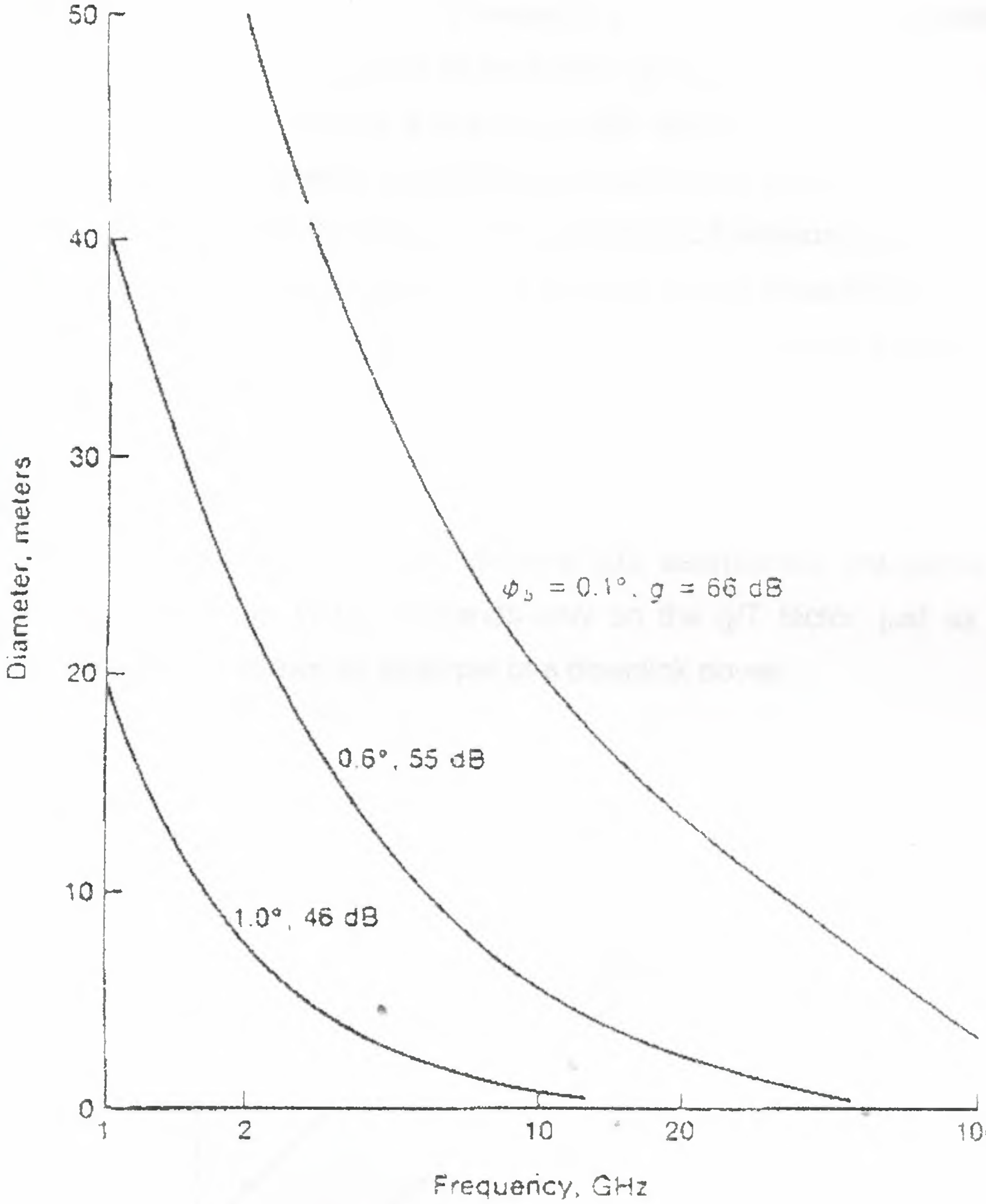

Figure 4.9 Earth-station antenna size versus frequency (Φ_b = half-power beam width, g = gain, ρ_a = 1)

g/T°. Even with significant range losses (≈200dB) and relatively low g/T° values, an acceptable uplink communication link can usually be established.

4.4.2 Satellite downlink

A satellite downlink (Figure 4.10a) is constrained by the fact that the power amplifier and transmitting antenna must be space borne. This limit the power amplifiers to the efficient, lightweight devices, with limited output power capabilities that are dependent on the carrier frequency (see figure 4.10b). The spacecraft antenna, while similarly limited in size, must use beam patterns that provide the required coverage area on Earth. Recall that the coverage area for a specified minimal viewing elevation angle depends only on the satellite altitude. Hence, the satellite downlink beam width for a given coverage area is automatically selected as soon as the satellite orbit altitude is selected. This also means the corresponding downlink antenna gain is established by the orbit altitude. By using higher-frequency bands (smaller λ), this required downlink beam width can be achieved with smaller satellite antenna sizes, as stated before. Spacecraft antennas that provide the maximal coverage area are referred to as global antennas.

With satellite power level and antenna gain established, the carrier power collected at the earth station depends only on the g/T factor, just as for the uplink. Figure 4.11 shows an example of a downlink power

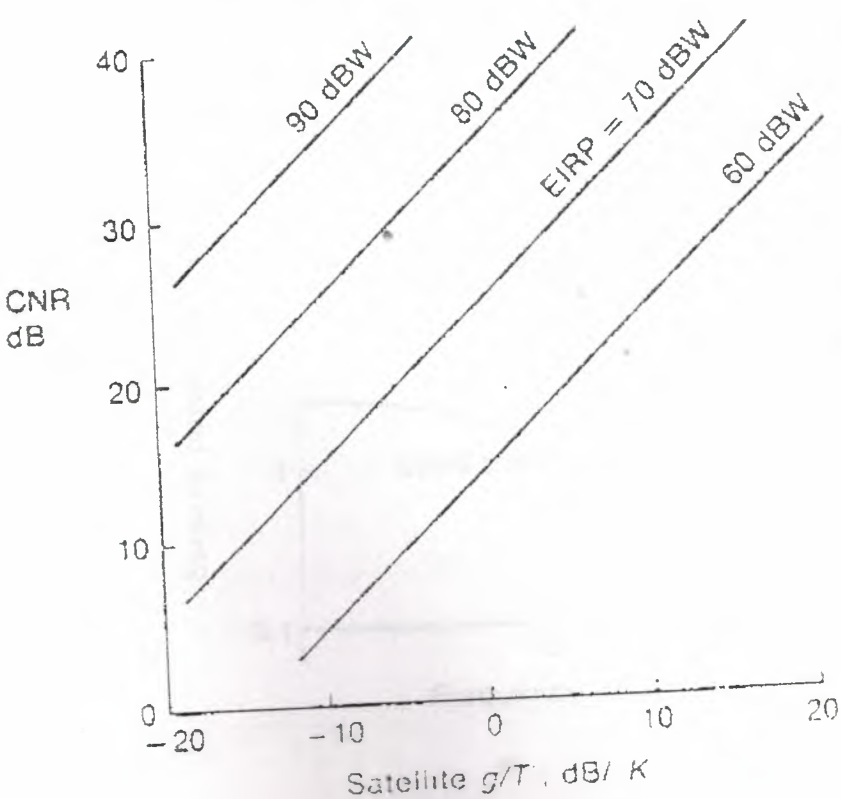

Figure 4.10 Uplink CNR versus satellite g/T° C-hand link, bandwidth =10 MHz; link parameters

budget for a 10-MHz bandwidth and global satellite antennas, and again generalizes to a CNR plot in terms of satellite power and receiver g/T°. It is evident that relatively large earth-station g/T° is needed to overcome the smaller EIRP of the satellite. This means small earth station will be severely limited in their ability to receive wide bandwidth carriers.

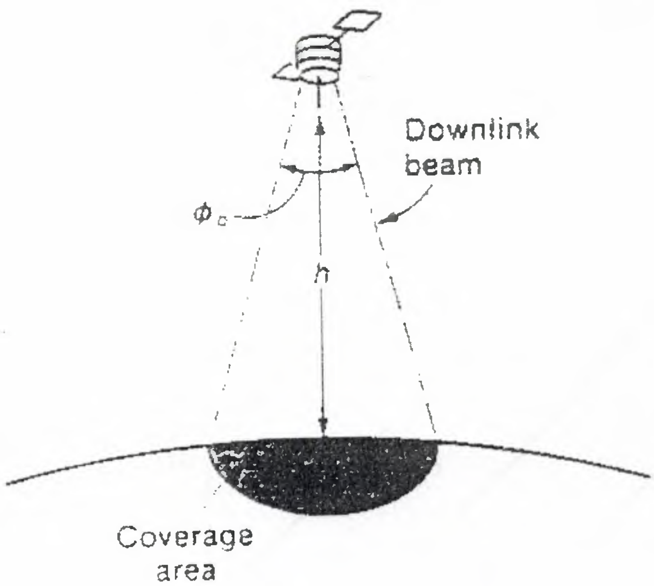

a.

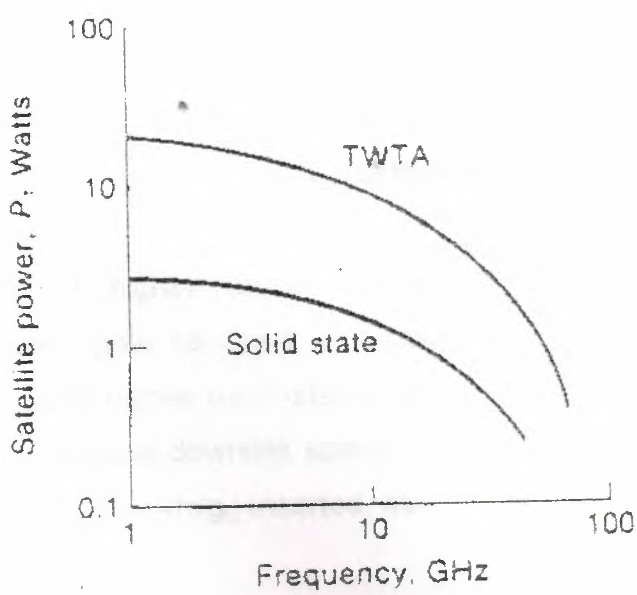

b.

Figure 4.11 Satellite downlink: (a) model: (b) spacecraft power sources

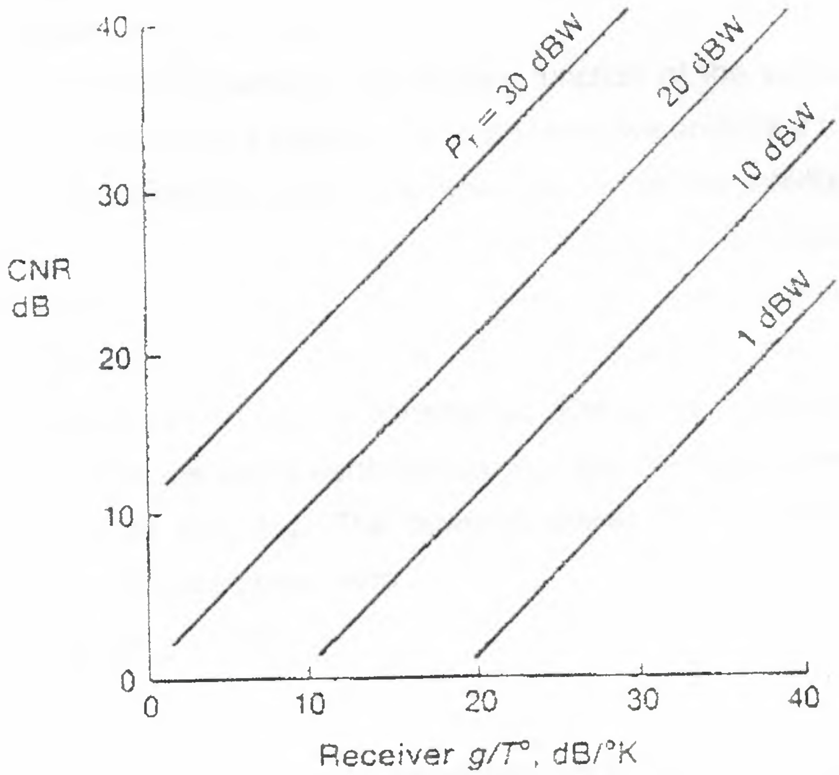

Figure 4.12 (a) Downlink C-band link budget, (b) Downlink CNR versus receiver g/T°. = satellite power, global antenna, bandwidth =10 MHz, link parameter

Although use of higher carrier frequencies allows smaller satellite antennas, care must again be used in accounting for its effect in downlink analysis, it will produce higher earth-station g/T values. but it will not increase CNR owing to the increased downlink space loss. To emphasize this point, with satellite beam width $\Phi 2b \cong (4\pi/g_t)$ inserted, as

$$CNR_d = \frac{P_T A_r L_a}{\phi_b^2 z^2 k T^\circ_{eq} B_{RF}} \tag{4.13}$$

With the terms in the denominator fixed by the link, we see that downlink CNR depends only on available satellite power P_T and on receiver collecting area A_r. Note that neither satellite E1RP nor receiver gain directly affects downlink quality. The choice of frequency band is, of course, important in determining available P_T (Figure 3.11b), and in determining atmospheric losses. A secondary consideration in frequency band selection is the possible advantage that may be attained by allowing wider RF bandwidths.

4.4.3 Repeater Link Analysis

In transponding satellites, the primary function of the spacecraft is to relay the uplink carrier into a downlink. In this section we analyze a transponder channel as a combined uplink-downlink, where we model the satellite simply as an ideal linear power amplifier. We neglect the frequency translation between uplink and downlink, and simply convert the former to the latter through an amplifier with power gain G (Figure 4.13). This represents the most basic, idealized, repeater link that can be constructed. The uplink power is composed of a signal term from the uplink earth station, P_{us}, and the noise power collected at the satellite front end, P_{un}. The downlink power P_T is composed of an amplified signal and noise power term

$$P_T = GP_{us} + GP_{un} \tag{4.14}$$

Let L represent the combined total power gain (or loss) in the downlink, including antenna gains and channel losses. From Eq. (4.5)

$$L = g_t L_a L_p g_r \tag{4.15}$$

Ideal amplifier

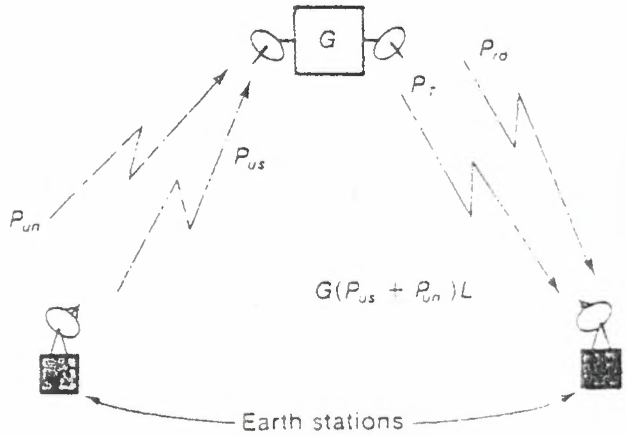

Figure 4.13 Combined up-down link repeater. (L = combined down-link losses)

The received downlink carrier power is then

$$P_{rs} = GP_{us}L \tag{4.16}$$

The retransmitted uplink noise appearing at the downlink receiver

$$P_{rn} = GP_{un}L \tag{4.17}$$

In addition, a noise power $P_{rd} = kT^{o}_{d}B_{d}$ appears at the downlink receiver due to its noise temperature T^{o}_{d} and bandwidth B_{d}. Hence, the combined CNR at the downlink receiver is

$$\mathrm{CNR}_d = \frac{P_{rs}}{P_{rn} + P_{rd}}$$

$$= \frac{P_{us}}{P_{un} + (P_{rd}/GL)} \tag{4.18}$$

Dividing by P_{un}, we have

$$\mathrm{CNR}_d = \frac{P_{us}/P_{us}}{1 + (P_{rd}/P_{rn})}$$
$$= \frac{(\mathrm{CNR}_u)(\mathrm{CNR}_r)}{\mathrm{CNR}_u + \mathrm{CNR}_r} \qquad (4.19)$$

where we have denoted

$$\mathrm{CNR}_u \triangleq \frac{P_{us}}{P_{un}} \qquad (4.20)$$

as the uplink CNR at the satellite, and

$$\mathrm{CNR}_r \triangleq \frac{P_{us}GL}{P_{rd}} \qquad (4.21)$$

as the downlink receiver CNR. This last CNR equation is based on satellite-transmitted carrier power and receiver noise only, that is, as if there were no uplink noise. Thus, even with a relatively simple and ideal satellite repeater model, we establish a basic property of repeater systems. The downlink CNR depends on both the uplink CNR and the receiver CNR, and can never exceed cither one. Thus, the weakest of the uplink and downlink channels will determine the performance level of a repeater system. Even with perfect repeater amplifiers, design of the uplink, as well as the satellite downlink, must be taken into account. Practical, conical satellite models, but with additional forms of degradations occurring. We point out that by inverting CNR_d we can rewrite Eq. (4.19) as

$$(\mathrm{CNR}_d)^{-1} = (\mathrm{CNR}_u)^{-1} + (\mathrm{CNR}_r)^{-1} \qquad (4.22)$$

This is sometimes more convenient to use in computing CNR_d in repeater analyses.

For a transponded digital link, the downlink CNR_d can be converted to E_b/N_o to determine bit-error probability for the linear amplifier satellite. This requires replacing B_d by $1/T_b$, and writing

$$\left(\frac{E_b}{N_0}\right)_d = \frac{(E_b/N_0)_u(E_b/N_0)_r}{(E_b/N_0)_u + (E_b/N_0)_r} \tag{4.23}$$

where $(E_b/N_o)_u$ and $(E_b/N_o)_r$, are obtained from Eqs. (4.20) and (4.21) by taking the noise bandwidth as $1/T_b$ Hz.

Note again that digital performance depends on both uplink and downlink CNR. Figure 4.14 plots PE in Eq. (4.24) for both these parameters, showing how the weaker of the two links determines the overall PE performance.

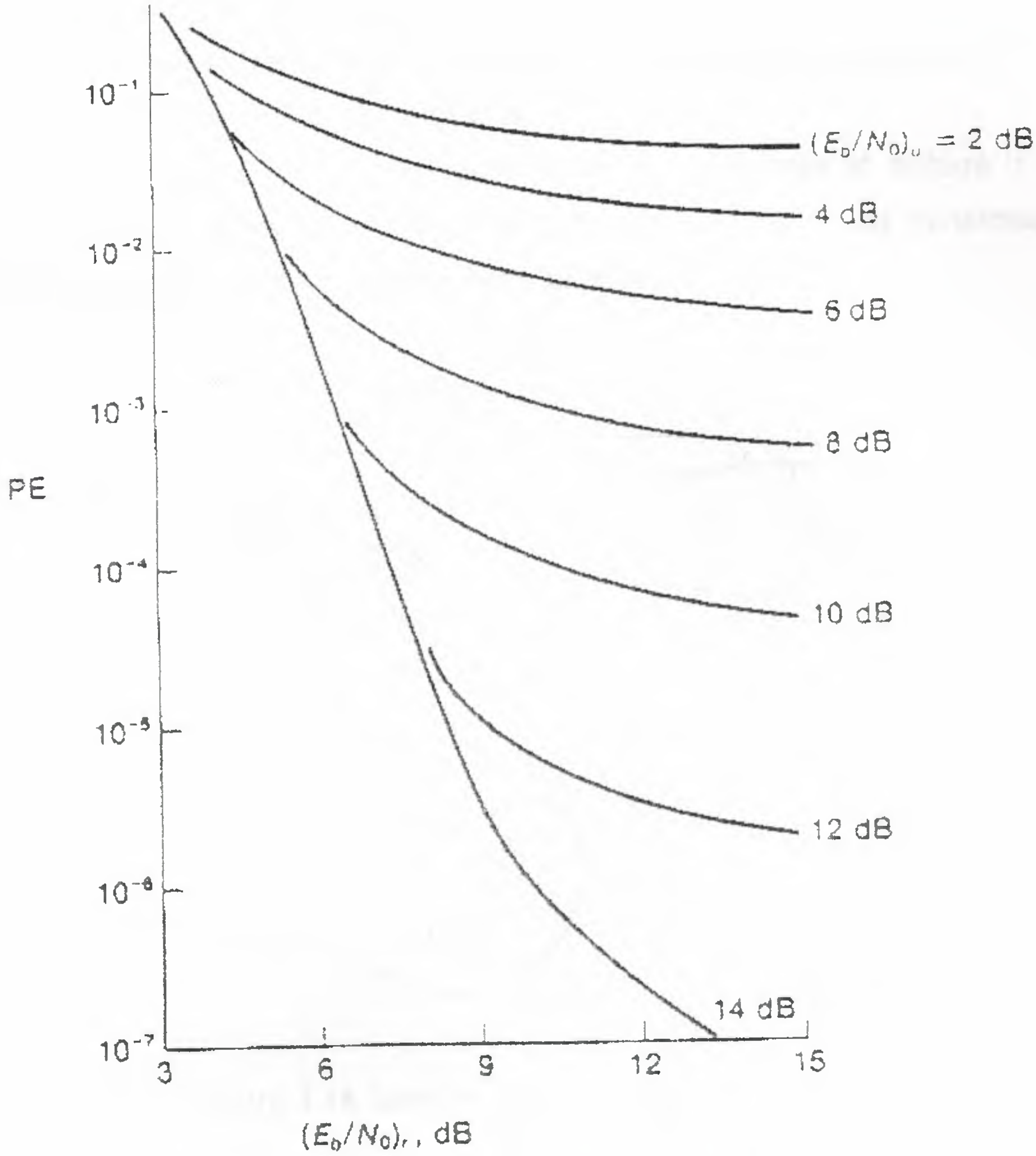

Figure 4.14 Bit-error probability, PE, for a BPSK up-down link. $(E_b/No)_u$ refers to uplink, $(E_b/No)_r$ to downlink

4.4.4 Satellite Cross links

Satellite systems often require communications between two satellites via a crosslink. A crosslink can be established between synchronous satellites, low-earth-orbiting satellites, or deep-space satellites. A crosslink between two orbiting satellites is referred to as an anti-satellite link (ISL). As a communication link, an anti-satellite link has the disadvantage that both transmitter and receiver are space borne, limiting operation to both low p_T and low g/T° values. To compensate in long links, it is necessary to increase EIRP by resorting to narrow transmit beams for higher-power concentration. With satellite antenna size constrained, the narrow beams are usually achieved by resorting to higher carrier frequencies. Hence, satellite crosslink are typically designed for K-band (20-30 GHz) or EHF (60 GHz) frequencies.

Consider the crosslink model in Figure 4.15. Two satellites at altitude h are separated by angle Φ_s as shown. The transmitting satellite has transmission power P_T available, and we assume both satellites use

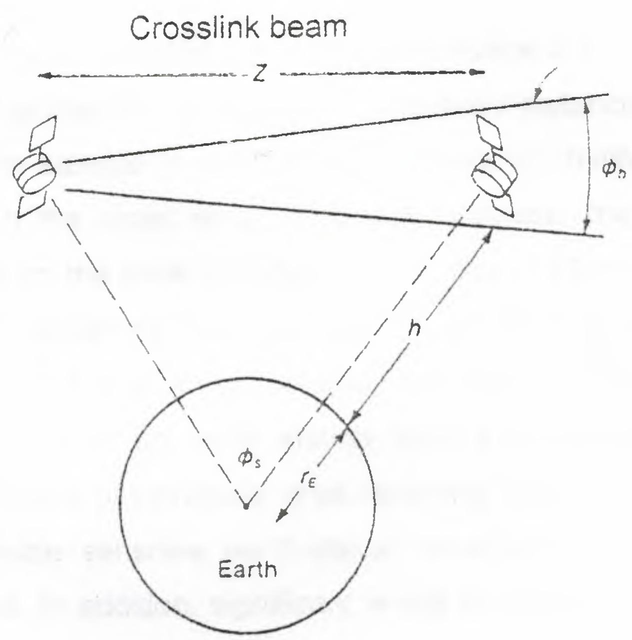

Figure 4.15 Satellite crosslink model

antennas of diameter d. The receiving satellite has noise temperature T°. The propagation distance between the satellites is given by

$$z = 2(h + r_E)\sin(\phi_s/2) \tag{4.24}$$

where r_E is the Earth's radius. The maximum line-of-sight distance occurs when

$$z_{max} = 2[(h + r_E)^2 - r_E^2]^{1/2} \tag{4.25}$$

which, for h » r_E , is approximately 2 h. We assume first that both satellite locations are known exactly by each, and each is perfectly stabilized, so that each satellite uses antenna beam widths Φ_b pointed exactly at each other. The

The transmitted beam width must be wide enough to encompass these pointing errors. This shows that a key element in crosslink systems is the ability to point between satellites. It is evident that a trade-off exists between reducing the crosslink beam (more concentrated power) and improving the pointing accuracy.

4.4.5 Deep-Space Links

A special type of satellite link is the deep-space link in which image and sensor data from unmanned spacecraft at planetary distances are transmitted to Garth. While the satellite links considered previously involved transmissions over distances on the order of synchronous altitudes, the deep-space link involves distances on the order of astronomical units (1 AU = 1.5 x 10^8kin). The combination of the extremely long propagation paths, along with constraints on spacecraft size, weight, and power, severely limits the available receiver power that can he collected at an earth station from an interplanetary probe. To compensate, a network of extremely large receiving dillies (≈ 60 m) are located worldwide to provide sensitive earth-station reception with minimal ground-based interference. In addition, significant levels of coding and error correction arc inserted to improve the link performance. Planetary probes have successfully been completed since the 1960s. Data rates from deep space have increased from a few bits per second with the early Moon and Venus probes, to hundreds of kilobits per second for the Jupiter probes of the 1980s.

Communications were the weak signal the frequency bands allocated specifically for deep-space research and strengths of the return link and the high-power transmissions needed for the forward command and ranging links to the vehicle, these bands are carefully monitored and reserved to ensure complete restriction to deep-space operations. These particular bands were selected for optimal communication performance, minimal propagation effects, available efficient hardware, and compatibility with existing terrestrial systems. The deep-space bands are subdivided into individual channels that are assigned specifically for each space mission. Primary use is made of the 2-GHz and 8-GHz bands, with future applications planned for the K-band frequencies.

Space vehicles invariably use turnaround ranging systems continually to monitor location and velocity throughout the mission. This requires that the forward carrier frequency must be translated by a fixed, precise factor at the spacecraft to generate the coherent return carrier. Hence, the forward and return frequencies selected for any deep-space mission must be an exact ratio. For example, the return carrier in the 2-GHz band is always selected to be exactly 240/221 times the forward carrier.

Modulation on the transmitted carriers involves the combination of the ranging waveform and the data or command sub carriers, which are then phase-modulated on the carrier. In the forward link the ranging waveform and command sub carriers are separated after phase demodulation at the vehicle. The recovered ranging signal is then instantaneously returned by adding to the data sub carrier and remodulating onto the return carrier. At the ground-tracking station the returned ranging waveform is processed for two-way ranging and Doppler estimation, whereas the data sub carrier is separated and decoded to recover the spacecraft probe, sensor, or video information. Excessive coding is inserted to aid the link performance, but the resulting link margin is still somewhat low, requiring accurate and precise control of link losses to complete the telemetry link. Often, diversity reception usingcamer reinforcement from other ground stations can be inserted to help improve the link margin.

CONCLUSION

The telephone channel is essentially a linear, bandwidth-limited channel. The restriction on bandwidth arises from the requirement of sharing the channel among a multitude of users at anyone doe. A practical solution to the telephonic communication problem must therefore minimize the channel bandwidth requirement, subject to a satisfactory transmission of human voice.

Enormous potential bandwidths, resulting from the use of optical carrier frequencies around 2 X 10^{14} Hz; with such a high carrier frequency and a bandwidth thoroughly equal to 10 percent of the carrier frequency, the theoretical bandwidth of a light-wave system is around 2 X 10^{13} Hz, which is very large indeed.

In a mobile radio environment, we thus speak of a multipart phenomenon in that the various incoming radio waves reach their destination from different directions and with different time delays. Indeed, there may be a multitude of propagation paths with different electrical lengths, and their contributions to the received signal could combine in a variety of ways.

Insignificant sky background noise; the sky background noise reaches its lowest level between 1 and 10 GHz. In the 6/4-GHz band, a typical satellite is assigned a 500 MHz bandwidth that is divided among 12 transponders on board the satellite. Each transponder, using approximately 36 MHz of the satellite bandwidth, corresponds to a specific radio channel. A single transponder can carry at least one color television signal, 1200voice circuits, or digital data at a rate of 50 Mb/s.

REFERENCES

[1] Mamedov F.S., Telecommunication, Lecture notes, Near East University Press, Nicosia, 2000.

[2] Simon Haykin., Communication Systems, 3^{rd}ed., John Wiley & sons Inc, 1994.

[3] Lee W.C.Y., Mobile Communication Engineering, McGraw-Hill, 1982.

[4] C.Sandbank., OPTICAL Fiber Communication Systems, John Wiley & sons Inc, 1980.

[5] Ippolito, Jr., Radio wave Propagation in Satellite Communications, Van Nostrand Reinhold, 1986.

[6] Simon Haykin., Digital Communications, John Wiley & sons Inc, 1988.